JOURNAL OF GEOPHYSICAL RESEARCH, VOL. 108, NO. E4, 8036, doi:10.1029/2002JE001888, 2003

Subsurface investigation of a rock glacier using ground-penetrating radar: Implications for locating stored water on Mars

John J. Degenhardt Jr.

High Alpine Research Program (HARP) and Department of Geography, Texas A&M University, College Station, Texas, USA

John R. Giardino

High Alpine Research Program (HARP), Department of Geology and Geophysics and Office of Graduate Studies, Texas A&M University, College Station, Texas, USA

Received 21 February 2002; revised 13 June 2002; accepted 25 June 2002; published 8 April 2003.

[1] The discovery of rock glacier-like features on Mars suggests the presence of flowing, or once-flowing, ice-rock mixtures. These landforms, which include lobate debris aprons, concentric crater fill, and lineated valley fill, hold significant promise as reservoirs of stored water ice that could be used as fuel sources for human exploration of Mars and provide a frozen record of the climatic history of the planet. To understand the deformation and distribution of ice within these landforms, fundamental descriptions of their internal structure and development are required. To this end, a ground-penetrating radar investigation was initiated using rock glaciers in the San Juan Mountains of Colorado as surrogates for similar Martian landforms. Results obtained from one of these rock glaciers show that the interior of the landform is composed of a layered permafrost matrix of ice, sediment, and ice lenses that comprise thicker depositional units formed through high-magnitude debris falls. Folds in the uppermost layers correspond to the surface expression of ridges and furrows, suggesting that compressive stresses originating in the accumulation zone are transmitted downslope through the rock glacier. Rock glacier features on Mars may also consist of layered permafrost, which would suggest a history of development involving seasonal frost accumulation and/or water influx from below. In terms of water storage within Martian analogs, consideration must include the possibility that some water ice may be stored in relatively pure form within lenses and vein networks such as observed in the surrogate rock glacier of this study. *INDEX TERMS:* 6225 Planetology: Solar System Objects: Mars; 6207 Planetology: Solar System Objects: Comparative planetology; 5470 Planetology: Solid Surface Planets: Surface materials and properties; 0925 Exploration Geophysics: Magnetic and electrical methods; *KEYWORDS:* Planetary geology, rock glacier, Mars, GPR, ground penetrating radar, viscous flow feature

Citation: Degenhardt, J. J., Jr., and J. R. Giardino, Subsurface investigation of a rock glacier using ground-penetrating radar: Implications for locating stored water on Mars, *J. Geophys. Res.*, *108*(E4), 8036, doi:10.1029/2002JE001888, 2003.

1. Introduction

[2] Rock glaciers are lobate or tongue-shaped bodies composed of mixtures of poorly sorted angular, blocky rock debris and ice. These landforms, whose wide distribution, occurrence, and significance often go unnoticed, move by slip, flow and/or creep deformation [*Giardino*, 1979; *Haeberli*, 1985; *Giardino and Vitek*, 1988a, 1988b] and have distinctive surface morphologies, including ridges and furrows perpendicular to flow direction. They generally occur in dry, continental areas rather than humid regions, perhaps because thin to absent snow cover and reduced glacier extension favor the existence of periglacial permafrost conditions and, hence, the preservation over long time intervals ground ice - a primary condition of rock glacier formation [*Humlum*, 1997]. Ages of rock glaciers range from incipient rock glaciers on Pico de Orizaba volcano [*Palacios and Vazquezselem*, 1996] through forms associated with the Little Ice Age [*Humlum*, 1996], to features several thousand years old [e.g., *Kaeaeb et al.*, 1997; *Calkin et al.*, 1998], to relict rock glaciers that formed during and at the end of the last Ice Age ~18,000–10,000 years BP [*Sandeman and Ballantyne*, 1996; *Humlum*, 1998]. Direct dating of rock glaciers using pollen analysis and C^{14} ages of moss has recently been provided by *Haeberli et al.* [1999]. The occurrence of past or present glaciers is not necessarily a prerequisite to the formation of rock glaciers because these landforms exist in both glacial and nonglacial areas [*Giardino*, 1979, 1983; *Johnson*, 1983; *Haeberli*, 1985].

[3] Serious study of rock glaciers began with the seminal work by *Wahrhaftig and Cox* [1959], who put forth the idea

0148-0227/03/2002JE001888

that rock glaciers represent a landform continuum in the alpine environment. *Barsch* [1977] and *Giardino* [1979] later addressed the role of rock glaciers in terms of debris transport and found that rock glaciers account for approximately 60% of all mass transport in the alpine environment. Our current understanding of rock glacier deformation is outlined in the work of *Haeberli* [1985]. It is based on flow models adopted from studies of glaciers and limited physical data from rock glaciers around the world. Subsequent continuum-based [*Giardino and Vitek*, 1988a, 1988b], dynamics-based [*Johnson*, 1978, 1983], and form-based [*Corte*, 1987] classification schemes have also been developed.

[4] Although the geomorphology of lobate landforms with surficial ridges and furrows perpendicular to flow direction is well documented, our current knowledge of their movement mechanics and flow behavior is based on limited data obtained exclusively from terrestrial rock glaciers. Knowledge of the internal composition and fabric is necessary to understand the flow dynamics responsible for rock glacier deformation [*Fitzgerald*, 1994], but the difficulty and cost associated with direct observation of the internal characteristics make acquisition of these data problematic. For example, direct rheological measurements (i.e., flow direction, flow velocity, and stress fields) are time dependent and lengthy. To fully understand the movement and deformation patterns within rock glaciers, a fundamental (i.e., generic) description of their development is required. However, before the mechanics of motion can be understood, internal structure must be accurately identified.

[5] In this study, we identify the internal structure of a lobate rock glacier with characteristic ridges and furrows using ground-penetrating radar (GPR), a nonintrusive method of subsurface remote sensing. The investigation is directed at understanding the movement and deformation of ice-rich, slow mass-movement forms on Mars through the use of surrogate rock glaciers on Earth. The insights presented in this paper have been developed through a process of: (1) describing the internal structure of a lobate rock glacier, (2) developing a model for rock glacier development, (3) providing a plausible explanation for the origin of transverse ridges and furrows, and (4) mapping water pathways within a rock glacier. The methodology established here can be applied directly to investigations on Mars where information about the distribution of stored ice within landforms is paramount.

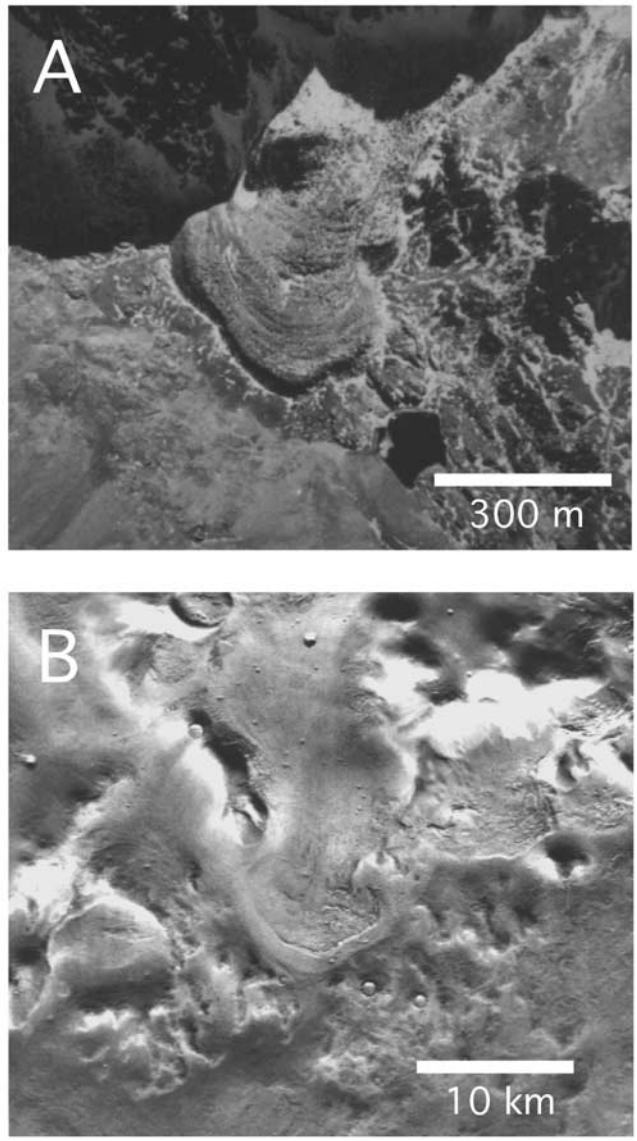

Figure 1. Lobate viscous-flow features on Earth and Mars; (a) Rock glacier located in the San Juan Mountains of Southwest Colorado, USA; (b) A landform on Mars resembling terrestrial rock glaciers. This feature, a lobate debris apron, is located in the northeast portion of the Hellas Impact Basin (Viking Orbiter Image 585-B09, courtesy of the Lunar and Planetary Institute, Clear Lake, TX).

2. Similar Features on Mars

2.1. Water Ice in Regolith

[6] On Mars, geomorphic features resembling rock glaciers (Figure 1) have been recognized as possible ice-rich bodies that have undergone viscous creep [*Lucchitta*, 1986, 1993]. Much of this ice may consist of frozen water, perhaps formed by recent or ongoing processes. This concept is supported by theoretical arguments of *Mellon and Jakosky* [1995], who suggest substantial quantities of ice exist in the near-surface regolith. Generally, the thin atmosphere of Mars forces the frost point of water to remain below 200°K. Thus, at higher temperatures, ice at the surface would sublime rather than melt. The regolith covering of these landforms may, however, provide sufficient insulation for the persistence of the ice within, particularly if the water ice is sealed off from the atmosphere by a continuous layer of frozen CO_2.

[7] The geographic distribution of viscous-creep features on Mars is consistent with the stability of ice as dictated by thermodynamic laws. *Farmer and Doms* [1979] provide a model for ice stability which suggests that in locations where temperatures in the top 10 meters of regolith exceed 198°K, ground ice will become unstable and can escape to the atmosphere by sublimation and diffusion. Using thermodynamic models, *Clifford and Hillel* [1983] and *Mellon and Jakosky* [1995] found that a zone of ground ice instability exists between ±30° latitude. This is consistent with mapping done by *Carr* [1986] that shows virtually no creep features within 30° of the equator.

[8] Viking images of the northern plains on Mars reveal the presence of lobate features with wrinkled surfaces associated with rift valleys and the peripheral margins of splash-form craters. These landforms, which include lobate debris aprons, lineated valley fill and concentric crater fill, have been interpreted as possible viscous ice-flow features [e.g., *Carr*, 1987; *Lucchitta*, 1993] derived from materials loosened from their original locations. The materials appear to have been transported generally down gradient by mass-wasting processes followed by accumulation and subsequent creep flow [*Squyres*, 1978].

[9] Lobate debris aprons are thick, topographically convex accumulations of debris at the base of escarpments. The surface of a debris apron slopes gently away from its source (e.g., the escarpment), and then steepens to form a distinct flow terminus analogous to the toe of a rock glacier. This morphology is a reliable indicator that deformation and flow have taken place throughout a significant thickness of the deposit [*Squyres and Carr*, 1986]. In terrestrial rock glaciers, a steep-crested toe indicates that the landform is currently active or was active in the recent past [*Giardino et al.*, 1987]. Some lobate debris aprons exhibit distinctive surface lineations that are both parallel and transverse to flow. These features bear striking resemblance to terrestrial rock glacier counterparts. Debris aprons that are confined in narrow valleys have been termed lineated valley fill. They appear to be composed of the same material as lobate debris aprons. Lobate debris aprons are very common in the fretted terrain separating the northern lowlands from the southern highlands between 280° and 250° longitude [*Colprete and Jakosky*, 1998]. Almost all of these types of features are restricted to a region between 50° and 80° latitude [*Squyres*, 1988].

2.2. Rock Glacier Analogs: Hellas Impact Basin and Region of Fretted Terrain

[10] The Hellas region (27.5°–42.5°S, 260°–275°W), dominated by the Hellas impact basin, is topographically and geologically diverse. The generalized geology, recently mapped by *Tanaka* [1995], includes Mid- to Upper Noachian-age (~3,900–3,500 Ma) Patera material to the north of the impact basin, basin rim units of late Noachian (~3,600 Ma) to the north and west, and dissected rim units of upper Hesperian (~2,400–1,800 Ma) and late Amazonian (~300–100 Ma) to the south and east of the basin. Farther south and east of the basin are ridges and plains materials of upper Noachian to late Hesperian age. The basin was formed during the early bombardment period (~3,900 Ma), but is relatively well preserved. It makes up the deepest and broadest depression on Mars (~9 km relief, ~2,000 km across). Volcanism and channel dissection have significantly modified large portions of the northeastern and southern parts of the basin rim.

[11] Large-scale examples of rock glacier-like features have been documented in the region surrounding the Hellas Impact Basin (Figures 2 and 3) and in areas of fretted terrain extending 25° in longitudinal width, centered on 40° N. latitude and 45° S. latitude. Concentric crater fill, observed on the floors and walls of craters, exhibit concentric patterns of ridges and troughs that result from compressional stress acting inward from the crater walls (Figure 3c). The concentric ridges are especially common in these forms, owing to the sharp transition in slope as materials flow down the walls of craters to the crater floors. The material also displays large-scale morphologic features and eolian etchings similar to those found on the other types of viscous flow bodies described in the preceding section. Some crater fill landforms appear to be "deflated", a characteristic observed in some debris aprons. In the southern hemisphere, lobate debris aprons are restricted to the mountainous terrains of the Argyre and Hellas impact basins (Figure 3). In the Hellas region, debris aprons are located mainly in the mountainous terrain on the eastern side of the basin. They are most common at the bases of escarpments and are less common as concentric crater fill [*Squyres and Carr*, 1984].

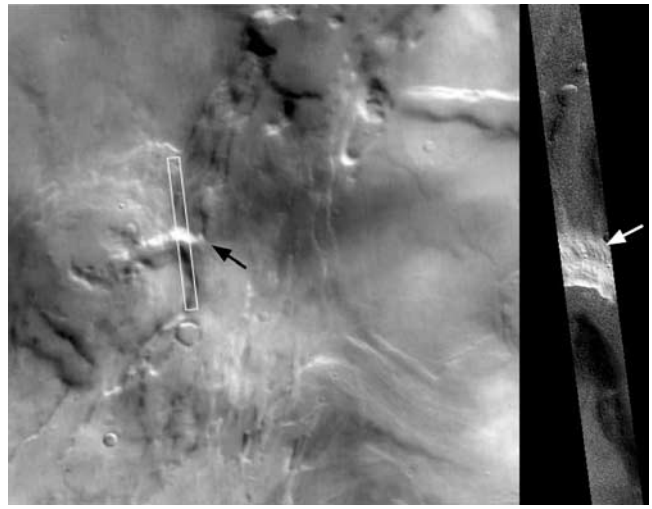

Figure 2. Mars Orbiter Camera image of a lobate debris apron located in a valley in the Tempe Terra region on Mars (black arrow). The narrow angle image (right) traverses the valley, which appears to dissect the wall of an impact crater. The debris that has accumulated at the base of the wall displays a wrinkled texture resembling ridges and furrows (white arrow). The area in the context image (M07-02045) is located at 47.29°N, 77.99°W and the narrow angle image scale is 2.40 km × 30.57 km (image M07-02044). Images courtesy of Malin Space Systems [*Malin et al.*, 2000].

3. Convergence of Investigative Approaches

3.1. Previous Methods of Investigation

[12] Researchers have used both direct and indirect methods in their investigations of rock glacier structure [*Burger et al.*, 1999]. Until recently, direct investigative methods included tunnels through rock glaciers [e.g., *Brown*, 1925], visual inspection of exposures, and shallow pits [e.g., *Wahrhaftig and Cox*, 1959]. *Potter* [1972] successfully used shovel and bulldozer pit excavations to investigate Galena Creek rock glacier and *Giardino* [1979] used a bulldozer excavation to study the structure of a rock glacier on Mount Mestas, Colorado.

[13] Coring methods must negotiate the difficult surface debris as well as interior heterogeneity. Mechanically operated drills have proven to be effective in penetrating both rock and ice by changing drill bits to meet encountered conditions [e.g., *Haeberli et al.*, 1988]. *Clark et al.* [1996] used a lightweight, hand-operated auger for studies of

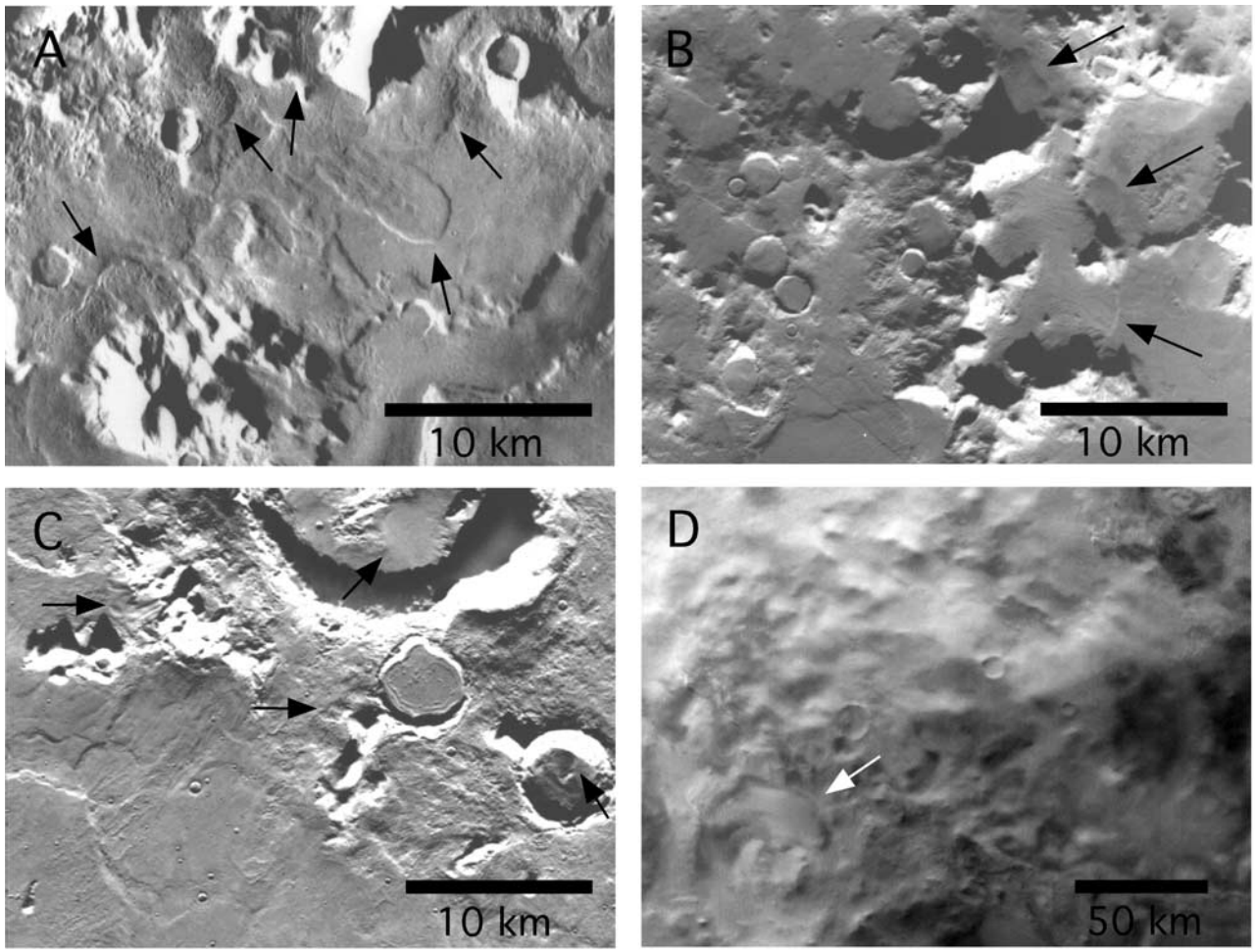

Figure 3. Viscous flow features located in the East and Northeast regions of the Hellas impact basin (27.5°–42.5°S, 260°–275°W). (a and b) Viking images of the northern plains showing lobate features with wrinkled surfaces and lineated flow patterns; (c) Concentric crater fill in the peripheral margins of splash-form craters; (d) Mars Orbiter Camera image of a viscous-flow feature resembling a rock glacier. Image numbers for (a–c) are 408S15, 412S82, and 412S16. The Orbiter Camera image is M19-01420, located at 47.47°S, 299.57°W [*Malin et al.*, 2001].

Galena Creek rock glacier (i.e., massive ice). The tool was useful at this locality because the volcanic source rock breaks into small clasts, making hand excavation of the debris feasible. During the summer of 1997, Giardino and Degenhardt were able to extract ice cores from the Yankee Boy rock glacier in the San Juan Mountains of Colorado. Such coring is no longer permissible in this area owing to increased government restrictions on sampling, equipment use, and the addition of new areas designated as national forest. Most of the techniques outlined above are also impractical for many localities where investigation is restricted by resources and accessibility. Large clast sizes and thick debris cover on rock glaciers challenge many investigations.

[14] Indirect methods include geophysical surveys, such as seismic refraction, gravimetry, resistivity, radio echo surveys, and ground-penetrating radar. In contrast to the labor- and time-intensive direct methods, geophysical methods allow relatively rapid and inexpensive acquisition of three-dimensional data for a rock glacier. Seismic refraction and resistivity surveys are the most commonly applied geophysical techniques. According to *Haeberli and Vonder Müehll* [1996], surface layer seismic velocities, typically ranging from 300 to 1,000 m/s contrast sharply with velocities from the top of ice-bearing layers. This contrast, which roughly parallels the surface of the rock glacier, can be traced along its length and is readily interpreted as the refractor representing the top of frozen sediment. Ice-supersaturated frozen material has an average seismic velocity of 3,500 m/s and a seismic velocity range of 2,000 to 4,000 m/s (indicating a degree of heterogeneity). Electrical resistivity, which is dependent on ice content and type, ranges from 1 to 10,000 kΩm in frozen sediments [*Haeberli and Vonder Müehll*, 1996]. Ice at marginal permafrost conditions has low resistivity (5–500 kΩm); massive ice has much higher resistivity (1,000–2,000 kΩm). Recent gravimetry applications at the much-studied Murtèl-Corvatsch rock glacier were successful, but required an intense modeling effort to correct for surrounding topography. Existing data were also extensively used to develop the model [*Vonder Müehll and Klingelé*, 1994].

[15] Few results from the use of geophysical methods mentioned in the previous paragraphs have been verified by

drilling or other methods to determine "ground truth," and few results except the depth of the boundary between an unfrozen surface layer and frozen material below are unequivocal. General limitations of these geophysical techniques sometimes include complex modeling efforts that can produce nonunique models and may require additional ground-truthing data collection. Based on these limitations, a more practical method of subsurface remote sensing is needed for rock glaciers. Ground-penetrating radar now provides a low-cost, accurate alternative to standard seismic techniques, without noise and disturbance to the environment.

3.2. Application of GPR to Rock Glaciers

[16] Ground-penetrating radar (GPR) is a relatively recent development [*Morey*, 1974; *Annan and Davis*, 1976; *Ulriksen*, 1982; *Daniels et al.*, 1988], having reached user practicality in the mid-1980s. This technique offers the sophistication of other geophysical techniques combined with portability and ease of use. It is ideally suited to applications in the alpine, where logistics and associated expense are usually prohibitive. GPR has been used effectively in a variety of geologic and geomorphologic environments including karst, glacial, periglacial, fluvial, and wetlands [e.g., *McMechan et al.*, 1998; *Murray et al.*, 1997; *Horvath*, 1998; *Roberts et al.*, 1997; *Jol and Smith*, 1995].

[17] Digital GPR profiles are generated using transient reflections of electromagnetic energy (EM) [*Daniels et al.*, 1988] and are similar in appearance to standard seismic profiles [*Daniels*, 1996]. EM in the frequency range of 10–1,000 MHz is transmitted into the ground in the form of short pulses. Profiles are generated from the return of radar signals as a portion of the transmitted energy that is reflected back to the surface as a result of changes in bulk electrical properties of the underlying materials [*Smith and Jol*, 1997]. Such changes in electrical properties can be attributed to sedimentological variation (i.e., changing grain size), facies changes, differences in state of materials (i.e., water-rock or water-ice contacts), mineralogy, and density. Resolution of GPR at 100 MHz (assuming a velocity of 0.1 m/ns) is ~0.25–0.50 m, which is ~10 times greater than conventional high-resolution shallow seismic sounding [*Smith and Jol*, 1997].

3.2.1. Investigation of a Surrogate Rock Glacier: Yankee Boy Basin, Colorado

[18] At present, indirect evaluations of landforms exhibiting viscous flow properties focus on rock glaciers with 'wrinkled' surface textures. This requires that primary consideration be given to those rock glaciers having prominent transverse ridge and furrow structure. Abundant examples of such rock glaciers can be found in the San Juan Mountains of Colorado. The rock glacier chosen for this investigation exhibits many morphologic characteristics (i.e., transverse ridges and furrows, lobate form, oversteepened toe, proximity to a headwall) that make it desirable for use as a surrogate for similar landforms on Mars. It is located in Yankee Boy Basin between Ouray and Telluride, Colorado.

[19] Yankee Boy Basin is a series of compound cirques defined by a sharp aretè extending from Gilpin Peak to Mt. Sneffels. The basin consists predominantly of Tertiary volcanics underlain by a block of Precambrian quartzite [*Luedke and Burbank*, 1976]. Mountain peaks that flank the basin are composed of San Juan volcanics, including Gilpin Peak tephra deposits, the Picayune Formation and the San Juan Formation. The Picayune Formation consists of a series of flows, breccias and tephra layers of intermediate composition and the San Juan Formation is mainly bedded tephra deposits of felsic composition. In the area of Mt. Sneffels, and along the northern edge of the basin, the mountains also include cores composed of older granodiorite and gabbro stock containing Precambrian quartzite inclusions. Quaternary deposits comprising the San Juan Formation cover most of the basin floor with limited exposure of the granodiorite and gabbro stock. The easily eroded bedrock supplies the parent material for deposits such as rock glaciers, alluvium, glacial drift, and landslide deposits. Holocene talus deposits occur at the base of most valley walls and rock glaciers typically occupy the heads and valleys of cirques. The rock glacier at the head of Yankee Boy Basin is shown in Figure 4.

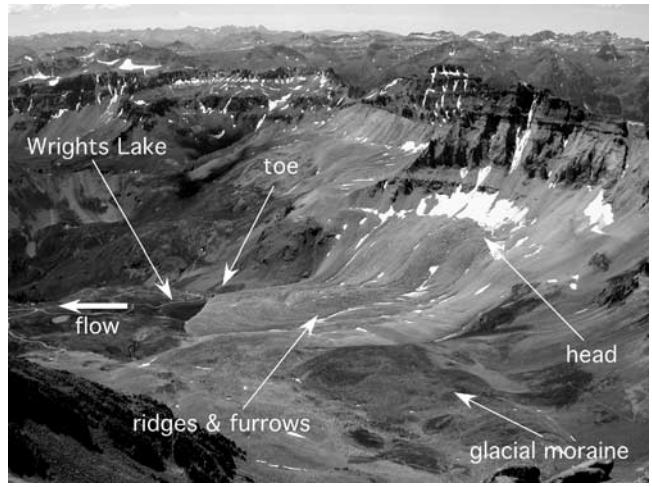

Figure 4. Yankee Boy Basin rock glacier, located between Ouray and Telluride in the San Juan Mountains of southwest Colorado. Photo was taken from atop nearby Mount Sneffels, a 4,328 m (14,150 ft) peak. The rock glacier is approximately 500 m (1,640 ft) long from the snow line to the toe at Wright's Lake, and 300 m (984 ft) wide at the middle. The rock glacier flows down a cirque that is bounded on the southwest side by Gilpin Peak ridge (4,174 m), seen in the background.

3.2.2. Equipment and Techniques

[20] A PulseEKKO™ 100A radar system from Sensors & Software, Inc. (Mississauga, Canada) was used in perpendicular broadside reflection mode with a constant source-receiver offset. Data for individual transects were collected using 2-m and 4-m source-receiver offsets for 50 MHz and 25 MHz (center frequency) antennae, respectively. For these configurations, 0.5-m and 1-m step intervals were used. On all profiles, the horizontal scale is distance in meters (m), and the vertical scale is presented as two-way travel time in nanoseconds (ns; right side of profiles) and depth in meters (m; left side of profile). Profiles were acquired with a 1,000 V transmitter and stacked 64 times with a time sampling rate of 800 ps. The profiles were processed and plotted in wiggle-trace and gray scale formats using PulseEKKO™ software.

[21] The raw 25 MHz reflection data were first processed using a correction for signal saturation (DEWOW). This correction reduces the easily diffused low frequency component of the radar signal through high-pass filtering. The DEWOWED data were then filtered using automatic gain control (AGC) at GMAX = 500, and loss-pass filtered at 20% for spatial correction. To accentuate amplitude variations, the processed data were bandpass filtered (1,024 PT FFT) at frequencies of 10, 20, 30 and 40 MHz to remove noise. Processing of the 50 MHz data was similar to that accomplished for the 25 MHz data with the exception that bandpass filtering was performed for frequencies of 20–50 MHz and 60–80 MHz. Laser surveying equipment was used to collect elevation data along the GPR transect lines. Topographic corrections were applied to the profiles prior to filtering.

3.3. Data and Interpretations

[22] The locations of the GPR transects were chosen for the purpose of identifying the gross morphologic and hydrologic characteristics of the rock glacier and for determining if a link can be established between internal structure and surface morphology. To measure the thickness of the rock glacier and to identify the internal structure (i.e., the nature and distribution of ice therein), a 440-m longitudinal transect (A-A′) was made parallel to the long axis of the rock glacier using the 25 MHz antennae. The transect line, which extends from the midpoint of the head area to the end of the toe, was routed over a prominent set of well-defined ridges and furrows on the youngest of the central flow lobes (Figure 5).

[23] Figure 6 shows the longitudinal profile prior to topographic correction. The data were spatially filtered at 20% and at 15% to determine the limit of processing that could be applied. At a filtering level of 20%, the reflection horizons are sharp and continuous, but a zone of 'ringing' is noticeable at the bottom of the profile (from 95–210 m). At 15%, the ringing was effectively removed. However, the reduced variation in amplitude throughout the remaining signal eliminated much of the contrast needed to clearly resolve individual reflection horizons. Thus, 20% spatial filtering was used for interpreting the profile. The two earliest continuous reflections represent air-wave and ground wave arrivals, respectively, and the strong continuous reflection at the bottom of the profile represents the limit of the velocity window and is not a feature detected in the subsurface.

[24] A noticeable feature of the topographically corrected profile (Figure 7) is the sharp change in slope of the reflection horizons where the steep accumulation zone (0–60 m) transitions abruptly to ridges and furrows (~60 m). This inflection (see Figure 5) marks a change in the slope of the cirque floor that corresponds to the onset of compression within the rock glacier. Reflection horizons in the accumulation zone are generally parallel to subparallel with the surface of the rock glacier. From 60–120 m (immediately beyond the inflection), the reflections are clear and continuous, and slant upward toward the surface of the rock glacier. Beyond 120 m, the reflections are generally parallel to the surface. It is significant to note that in the latter 320 m of the longitudinal profile, bends in the reflections strongly correspond to topography of the rock glacier where ridges and furrows are well pronounced. Reflections are continuous up to 100 m.

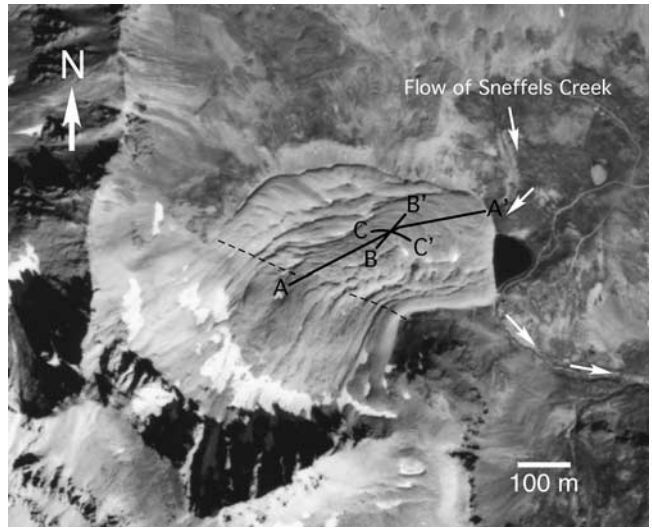

Figure 5. Aerial photograph of the Yankee Boy rock glacier taken in 1979 (37°59′N, 107°47′W). The image, cropped from a 9 × 9 inch 1:20,000 USDA photo, shows the rock glacier flowing down valley away from the headwall of the cirque. Cross section lines are shown for the radar profiles described in the text. Line A-A′ is 440 m long (25 MHz), and lines B-B′ and C-C′ are 90 and 75 m long, respectively. The latter were collected using 50 MHz antennae. The dashed line marks the inflection of the rock glacier. Small arrows indicate the flow path of Sneffels Creek, which runs through the toe of the rock glacier.

3.3.1. Velocity Determinations: Common Midpoint Profile

[25] A radarwave velocity of 0.12 m/ns was established for the rock glacier medium using a common midpoint (CMP) profile and semblance analysis (solution at 70 ns; Figure 8). The CMP, which was carried out along the first 40 m of transect C-C′ using 25 MHz antennae, was used for depth conversion and processing of the raw GPR data (Figure 9). The velocity value, which is slightly lower than those reported by *Isaksen et al.* [2000] and *Berthling et al.* [2000], likely represents frequency-dependent attenuation losses caused by the effect of fresh running water within the rock glacier. This reduction in velocity is expected to be greater at higher frequencies. To a lesser degree, dissipative losses by surface or volume scattering from heterogeneities on a scale close to the wavelength of propagation in the material may have been a factor. The pulse wavelengths (the product of frequency pulse period and velocity of the radarwaves) through the rock glacier medium, are 4.8 m and 1.8 m at 25 MHz and 50 MHz, respectively.

[26] Unpublished descriptions of shallow (7.6 m) drill core recovered from the frontal area of the Yankee Boy rock glacier in 1997 confirm the presence of alternating 0.5–1 m thick layers of coarse ice-rich and ice-poor layers. The layers are composed of blocks and platy clasts that are predominantly less than 0.5 m size in the largest dimension. The overall ratio of debris to ice ranges from 60–70% by volume, and some ice layers are comprised of up to 20–30% silts and fines. This is generally consistent with

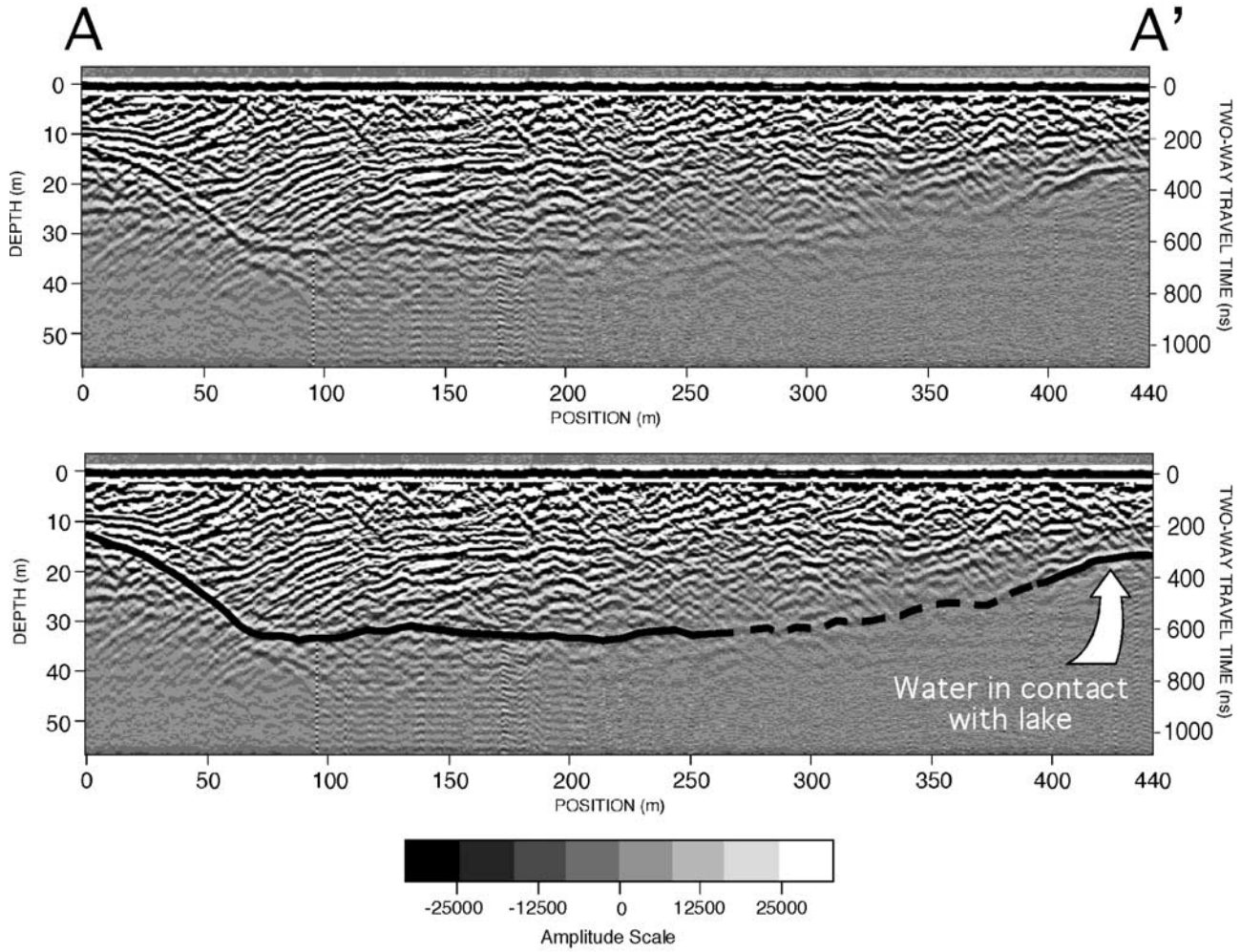

Figure 6. Longitudinal profile collected using 25 MHz antennae (uncorrected for topography). Line marks the contact between the rock glacier and the cirque floor. The inferred (dashed) portion of the line indicates a zone along the bottom where the radarwaves were attenuated by (running) water. The strongly coherent reflection in the last 50 m of the profile is interpreted to be collected water that is in hydrologic contact with Wright's Lake, which is located at the right end of the profile.

findings for drill core samples from other rock glaciers [*Haeberli*, 1985; *Barsch*, 1996].

[27] The theoretical vertical resolution of the radar signals was calculated using the equation [e.g., *Reynolds*, 1997]:

$$\lambda/4 = (V/F)/4 \quad (1)$$

where λ is the wavelength (m), V is the radarwave velocity of the medium (m/ns), and F is the center frequency of the antenna (MHz). Using the 25 MHz antennae, the theoretical resolution was calculated to be 1.2 m. Therefore, any layer visible on the radar profile has a thickness greater than one meter. The reflection patterns are consistent down to 700 ns ($\sim$45 m), which is the detectable limit of the radar achieved at this frequency. The 50 MHz antennae provided depth of penetration to 500 ns ($\sim$32 m) and resolution of 0.75 m, given a calculated theoretical vertical resolution of 0.60 m.

3.3.2. Hydrologic Character and Water Pathways

[28] The resolution and depth of penetration at 25 MHz was sufficient to identify the contact between the rock glacier and debris-covered cirque floor, as well as materials 5–8 m below the cirque floor. The contact reflection is strongly coherent from 0–190 m along the profile, beyond which diffusion (via attenuation) of the radar signal obscures the reflection patterns. In the last 50 m of the profile, the reflections are again coherent. We interpret the zone of diffusion, which reaches at least 5 m above the contact between rock glacier and cirque floor, to be a collection area for water residing in the downvalley portion of the rock glacier. The strongly coherent reflection in the toe area is interpreted to be a water table that is in contact with Wright's Lake. This contact is supported by the observation that water from nearby Sneffels Creek enters the toe of the rock glacier on the north side and exits the toe on the south side (see Figure 5). At the end of the GPR profile (440 m), this reflection horizon is estimated to be 7–8 m above the rock glacier-cirque floor contact. This corresponds closely to the level of Wright's Lake, which was estimated to rise 8 m on the oversteepened toe of the rock glacier. Together with meteoric waters, springs, seeps, and other water input

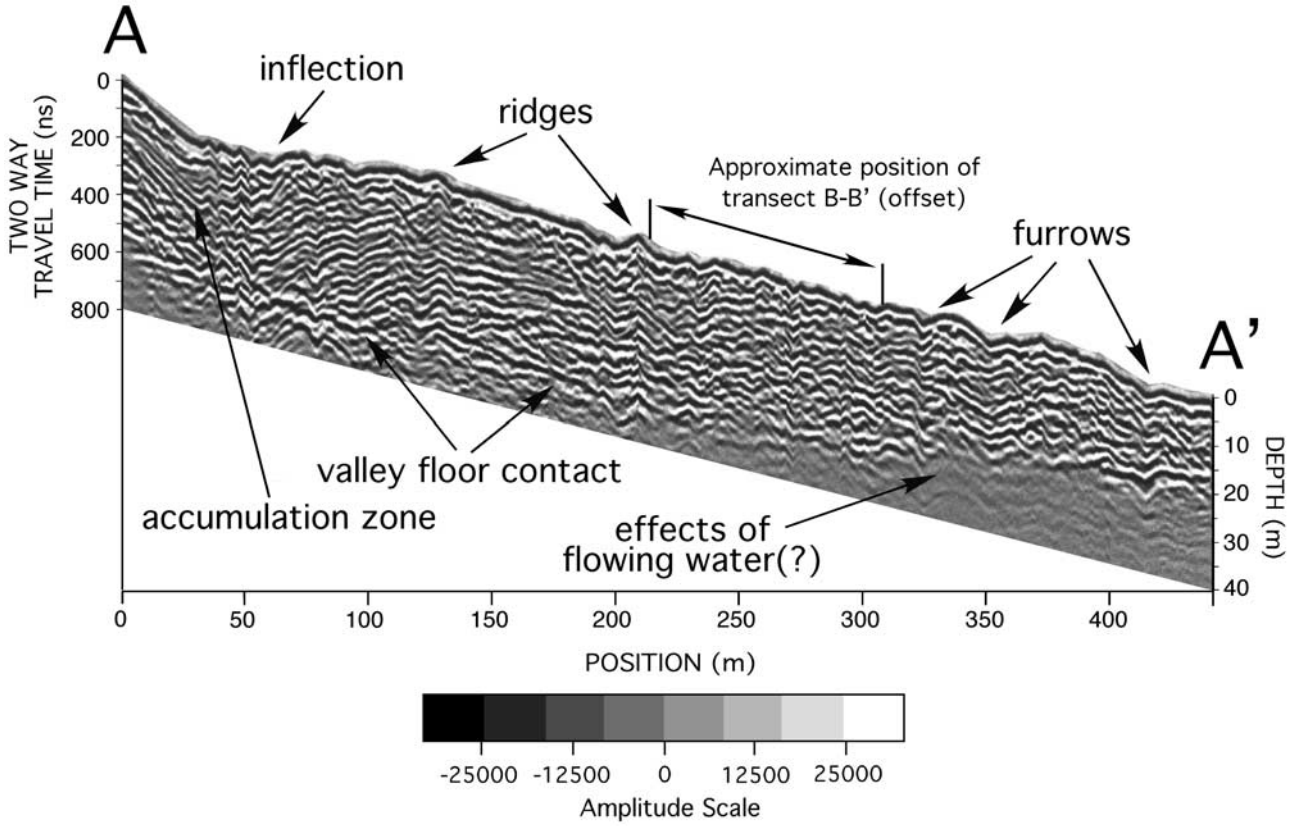

Figure 7. Topographically corrected 25 MHz longitudinal profile. Corrections were made to the profile in Figure 6 using laser survey data that was collected along the same transect line as the GPR survey. Note the relationship between undulations in the reflection horizons and surface topography. 'Processing' included 20% spatial filtering.

sources, the volume of water flowing in Sneffels Creek is more than sufficient to maintain a water table at the levels observed within the rock glacier during the summer months.

[29] In addition to the stored water, a network of water pathways was detected in the headward portion of the rock glacier. These pathways are identifiable in the longitudinal profile as intermediate range amplitude signals that do not conform to the characteristic horizontal reflection horizons (Figure 10). Such intermediate amplitude values are generated because the amplitude (and velocity) of radar waves are affected mainly by differences in the dielectric properties of the various phases encountered throughout the rock glacier (e.g., rock, ice and liquid water). Factors such as chemistry (i.e., salinity), state (liquid/gas/solid), distribution (pore space connectivity) and content of water also significantly affect the propagation of radar waves through the rock glacier medium. These effects are manifested in values of permittivity (the ability of a dielectric to store electrical potential energy under the influence of an electric field) for each of the phases. Fresh water (80 Farads/m) has a much higher permittivity than either freshwater ice (4 Farads/m) or granodiorite (~5 Farads/m). Thus, the observed ampli-

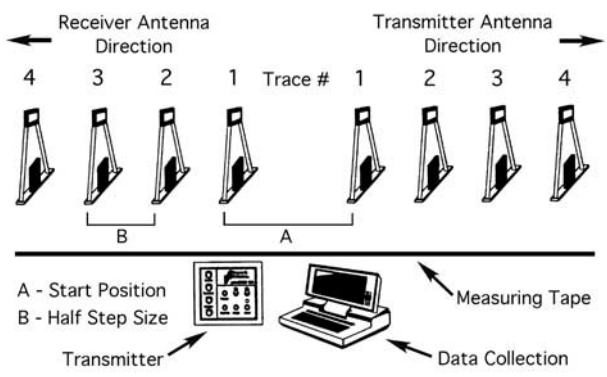

Figure 8. (opposite) Diagram illustrating the concept of collecting a common midpoint (CMP) profile for velocity determinations. The transmitting and receiving antennae are placed along a traverse perpendicular to the direction of movement. The antennae are moved at equal distance intervals (1/2 meter for 25 MHz antennae) from a common center point and separated until an average velocity value can be determined (using a representative, continuous reflection event in the profile), or when the maximum length of the fiber optic antenna cables is reached. The velocity value is determined by semblance analysis or by dividing the runout distance by the average two-way travel time for the given reflection horizon. This can be done by taking the inverse gradient of the reflection horizon as plotted on a T^2-X^2 graph [*Reynolds*, 1997]. Diagram modified from *Sensors & Software* [1996].

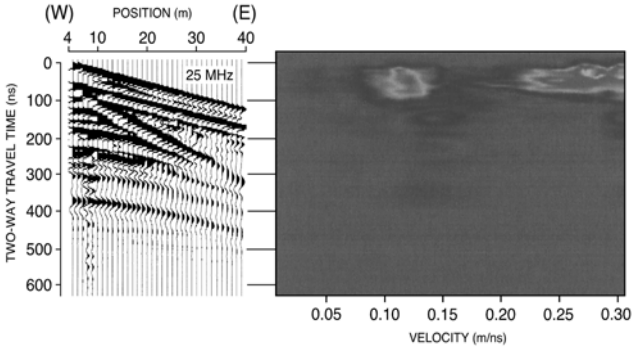

Figure 9. Common midpoint (CMP) profile used for determination of the representative radarwave velocity through the rock glacier medium. The profile was obtained at a frequency of 25 MHz with a 1000 V transmitter. A pulseEKKO™ 100A radar system from Sensors & Software, Inc. was used. The velocity value as determined from the semblance diagram on the right is 0.12 m/ns. The origin of the 'Position' axis is 4 m, which corresponds to the initial antennae separation at 25 MHz and the two-way travel timescale applies to the CMP profile and the semblance diagram.

tude variations can be attributed to the contrast between water and the solid phases of rock and ice.

[30] To test the validity of this means of detection, locations were recorded along the longitudinal transect where running water was audibly detected just below the surface of the rock glacier. The locations and estimated flow directions were then plotted on an enlarged portion of the longitudinal profile. The locations of running water detected on the surface of the rock glacier correspond closely to locations along the profile where branches of the water pathway network approach the surface (see Figure 10). The individual pathways, estimated to be 0.5–1.5 m in width, are in some places continuous from the surface of the rock glacier down to the cirque floor.

3.3.3. Ridge and Furrow Morphology

[31] To determine if ridge and furrow morphology is a manifestation of subsurface processes, two 50 MHz GPR transects were made on a section of the Yankee Boy rock glacier where ridge and furrow structure is prominent (see Figure 5). By providing greater resolution, these profiles were useful for interpreting the 25 MHz longitudinal profile described above. Profile B, a 90-m transect (B-B′, Figure 11), was made following a line oriented normal to ridges and furrows. The transect was located in close proximity to the 440-m longitudinal transect and rotated counterclockwise approximately 15° to maximize normalcy to the transverse ridges and furrows. Profile C, also collected using 50 MHz antennae, consists of a 75-m transect (C-C′, Figure 12) made along the top of a prominent ridge in the sequence. It trends in a direction orthogonal to Profile A and provides a perspective that is normal to the ridge axis.

[32] The 50 MHz radar results show that the internal structure of the rock glacier consists of parallel to subparallel layers of ice-rich and ice-poor strata. The laminated and overlapping character of the material is consistent throughout the sampling area and is continuous between profiles B-B′ and C-C′. This indicates that layering is continuous in the direction of ridge and furrow development as well as normal to it and implies that the layers were deposited by voluminous flows of rock debris that occasionally buried substantial amounts of snowpack on the surface of the rock glacier. The layering is deformed predominantly by folding, and fold fabric is evident throughout the entire thickness of the rock glacier. Minor faulting was also detected, mainly in the upper portions of the profiles. This aspect, however, does not appear to be the predominant mode of deformation within the rock glacier.

3.4. Contemporary Investigations

[33] To date, limited research involving the application of GPR to rock glaciers has been carried out [e.g., *Berthling et al.*, 2000; *Degenhardt and Giardino*, 2003; *Degenhardt et al.*, 2000, 2001; *Isaksen et al.*, 2000]. In a recent study, *Isaksen et al.* [2000] used GPR to investigate the composition, flow and development of two tongue-shaped rock glaciers in the permafrost of Svalbard, Norway. Using 50 MHz antennae, they obtained a 303 m longitudinal profile following the central flowline of the Hiorthfjellet rock glacier. The results show a clear reflection horizon to 15–20 m depth with reflections disappearing completely at 25 m. Along the profile line reflection horizons transition from parallel or slanting orientations relative to the surface, to horizons that dip upward in the mid-section (downslope) portions of the profile. These reflection horizons were interpreted to represent the end of a steep talus cone that

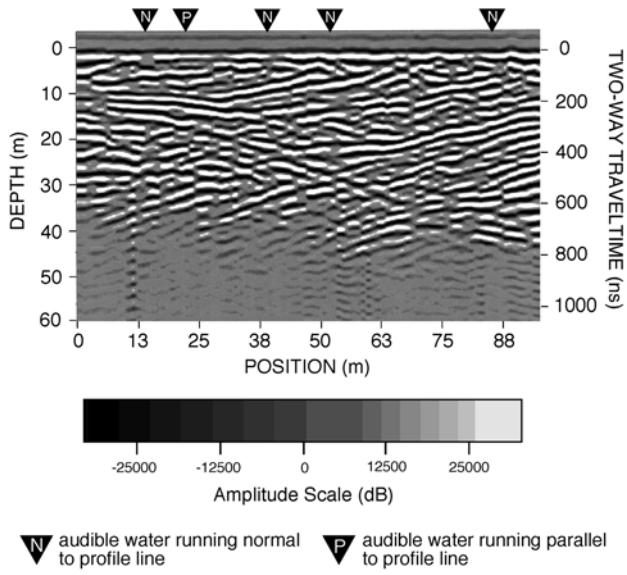

Figure 10. Radar profile of the first 94 meters of the longitudinal profile rendered in shades of black, white and gray to highlight amplitude variations corresponding to phase differences throughout the rock glacier. Alternating ice-rich and ice-poor layers are depicted in black and white. The network of gray colored lines is interpreted to represent flowing liquid water. The recorded locations of audible flowing water just below the surface of the rock glacier correspond well with locations where branches of the network meet the surface.

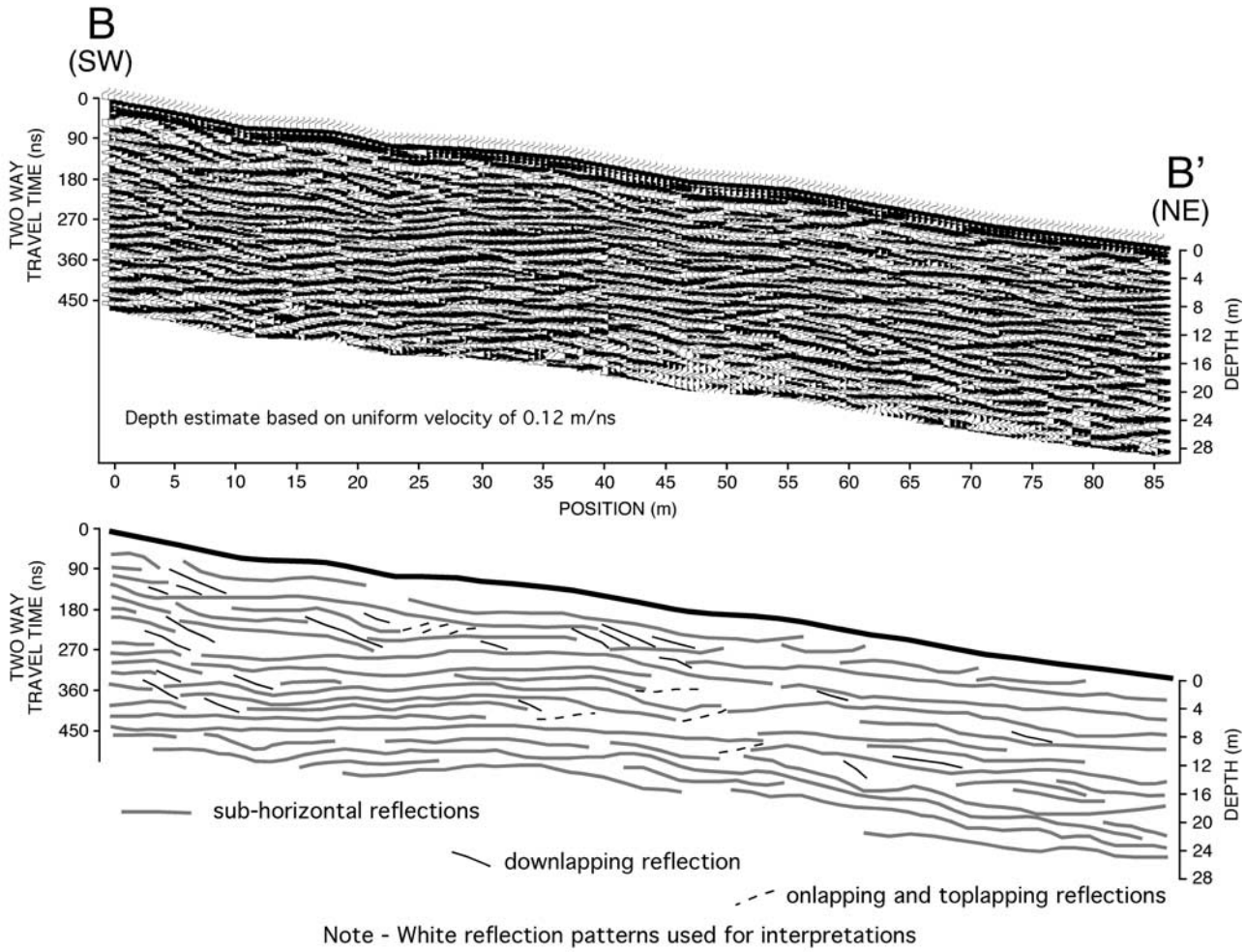

Figure 11. Topographically corrected GPR profile trending southwest to northeast along transect line B-B′ (Figure 5). Top: processed data without interpretations; Bottom: processed data showing interpretations based on mappable stratigraphic reflection horizons. Data was processed using software provided by Sensors & Software, Inc. Equipment included a 1000 V transmitter and 50 MHz antennae. A 2-m antenna spacing was used and data was collected using 0.5-m step intervals. The two earliest continuous reflections represent air-wave and ground wave arrivals, respectively.

marks a transition between the accumulation zone and the lower part of the rock glacier [*Isaksen et al.*, 2000]. Based on exposures in a lobate rock glacier near Longyeardalen, Norway, reflection horizons from the Hiorthfjellet rock glacier are believed to be caused by layers of ice alternating with layers comprised of fine material and blocks.

[34] In another study, *Berthling et al.* [2000] used GPR to investigate internal structures in four rock glaciers located in the continuous permafrost zone on Prins Karls Forland, western Svalbard. The longitudinal profiles obtained in that study revealed a system of reflectors that was comparable between the different rock glaciers. As observed in the Hiorthfjellet rock glacier, a layering structure parallel with the surface is visible in the upper parts of the profiles where the talus cones above the rock glaciers are located. Farther down profile, toward the rock glaciers, these reflectors are oriented at a slant against the surface slope. It was concluded that the layering formed by mass movements of higher magnitude that covered snow patches or the active layers above supersaturated permafrost.

[35] CMP velocities at Yankee Boy rock glacier are significantly lower than the 50 MHz values in the studies above. A velocity of 0.15 m/ns was obtained for the Murtèl-Corvatsch rock glacier [*Lehmann et al.*, 1998] and the Brøggerbreen rock glacier near Svalbard yielded a value of 0.14 m/ns [*Isaksen et al.*, 2000]. The low velocity values obtained in this study can be attributed to the presence of running (liquid) water throughout the Yankee Boy rock glacier, and to a lesser degree, by high attenuation in the conductive sand- and silt-rich ice layers that comprise the upper portions of the rock glacier.

4. Results: Implications for Landforms on Mars

4.1. Rock Glacier Development

[36] The pioneering work of *Wahrhaftig and Cox* [1959] suggested that rock glaciers formed by permafrost processes to create a frozen mixture of rock debris and ice within talus or morainal deposits. Since then, it has been found that rock glaciers occur as a physical response to three types of

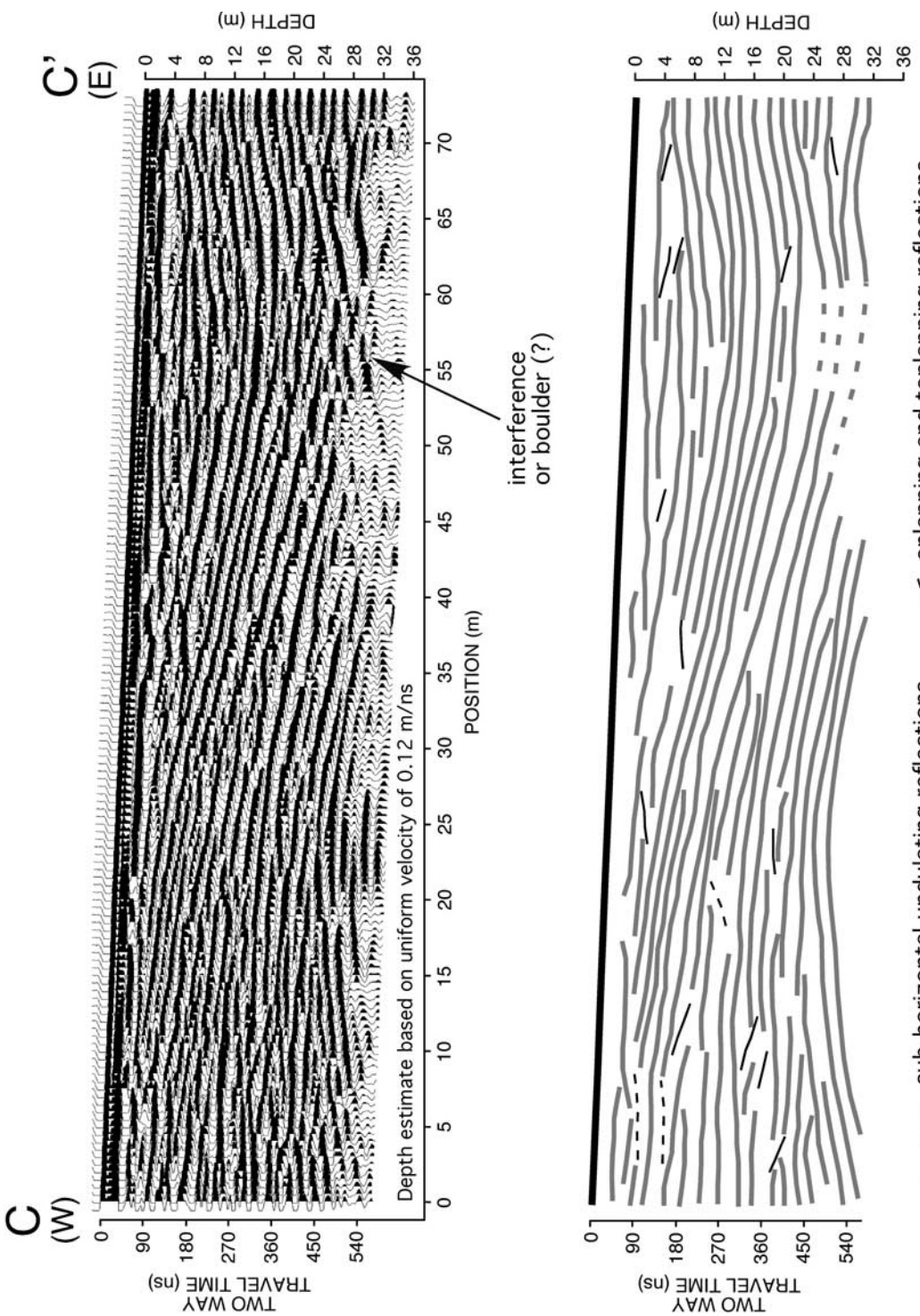

Figure 12. Topographically corrected GPR profile trending west to east along transect line C-C′ that runs along a single prominent ridge (see Figure 5). Top: processed data without interpretations; Bottom: processed data showing interpretations based on mappable stratigraphic reflection horizons. The concave folding in the right half of the profile is interpreted to represent infilling of a longitudinal furrow by overriding flow lobe materials. Equipment included a 1000 V transmitter and 50 MHz antennae. A 2-m antenna spacing was used and data was collected using 0.5-m step intervals. The two earliest continuous reflections represent air-wave and ground wave arrivals, respectively.

geomorphic processes: (1) glacial, (2) periglacial [*Johnson*, 1984], or (3) talus (as illustrated by *Shakesby et al.* [1987]). They often represent transitional forms in the landscape continuum, a geomorphologic concept developed by *Giardino and Vitek* [1988b] (Figure 13). With the advent of new technology and increased interest in recognizing and studying rock glaciers, these ideas have been affirmed and expanded through subsequent studies. A few of these studies provide evidence of thick massive ice in the rock glacier interior and suggest that these forms are debris-covered glaciers [*Potter*, 1972; *Whalley*, 1974; *Clark et al.*, 1994; *Whalley et al.*, 1994; *Potter et al.*, 1998] or forms that originated as perennial snowbanks or glacierets *Haeberli* [2000].

[37] Terrestrial rock glaciers are generally situated at the bases of massive, homogeneous and fractured cliffs and are rarely found where debris is finely crushed or where headwall fractures are excessively large [*Wahrhaftig and Cox*, 1959; *Evin*, 1987]. Source material is loosened by freeze-thaw action and transported by gravity downvalley or down escarpment, where it accumulates in locations of gradient decline [*White*, 1971]. A review of the general conditions for rock glacier formation has been given by *Corte* [1987]:

[38] (a) Relatively young mountain ranges having bedrock with rock mass properties (e.g., joint spacing, weathering characteristics, etc.) favoring the formation of blocky debris;

[39] (b) Microclimate conducive to daily freeze-thaw cycles or frost weathering, sufficient ground moisture for periglacial processes, low to moderate snowfall sufficient for production of debris and avalanche, and low insulating snow cover;

[40] (c) A combination of geographic position (e.g., latitude, elevation) and climate conditions (e.g., temperature, aspect) that promote periglacial processes and sustained subzero ground temperatures; and

[41] (d) Talus supply promoted by steep, rough terrain, perhaps by debris from a previous glaciation, frequent freeze/thaw cycles, and rock mass properties.

Precluding all of these is the existence of permafrost conditions (subzero mean annual ground temperature), which is the primary factor for rock glacier formation [*Haeberli et al.*, 1999; *Haeberli*, 2000].

[42] On Mars, the material that comprises the insulative cover for lobate debris aprons and valley fill is also thought to be the product of rockfall processes [*Lucchitta*, 1984; *Squyres*, 1988; *Carr*, 1995]. The production of regolith materials suitable for development of viscous flow features is largely attributed to meteorite impact, a process that played a major role in the structural evolution of the Martian crust [*Soderblom et al.*, 1974].

[43] Results of this GPR investigation show that the internal structure of the Yankee Boy rock glacier was formed by permafrost processes rather than by covering of remnant glacial ice. The distinct reflection horizons of the GPR profiles are discernable from the surface of the rock glacier to the bottom contact with the valley floor. These horizons depict the accumulation of snow/ice toward the upper reaches of the rock glacier and creeping permafrost where the valley slope decreases. We interpret these horizons to represent units of alternating layers of talus or rockslide debris and ice lenses and/or ice supersaturated sediments. The ice-rich layers are most likely formed by accumulation of seasonal snow, which is compacted upon burial by pulses of headwall debris (i.e., via large mass movement events), are buried and compacted. This mechanism of ice formation is believed to be the most important accumulation process for the rock glaciers investigated in Svalbard, Norway [*Isaksen et al.*, 2000; *Berthling et al.*, 2000]. Based on observations from limited amounts of recovered drill core and from GPR profiles generated in this study, the overall volume of ice comprising the Yankee Boy rock glacier is 30–40%.

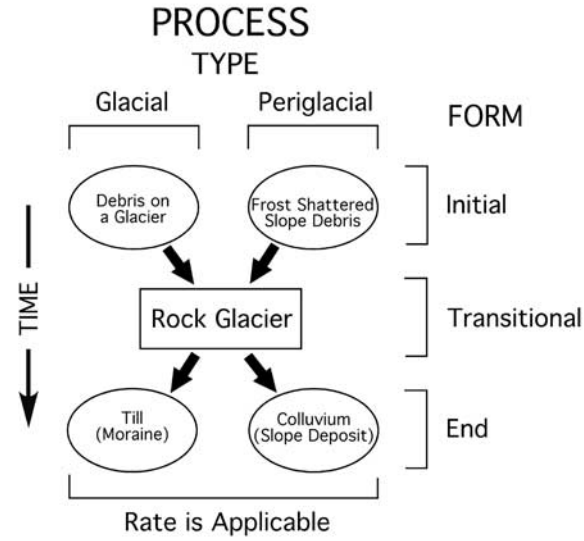

Figure 13. Diagram illustrating the alpine landscape continuum (modified from *Giardino and Vitek* [1988b]). Rock glaciers are transitional forms that can develop from two distinct processes and can progress to two distinct end-members. Rate of movement is related to process, not form.

4.2. Ice Sustainability and Flow

[44] For ice to be sustained within a dynamic (creeping) landform, minimizing the amount of insulation is required to reduce ablation of the permafrost (cryolithospheric ice). *Haeberli et al.* [1998] found that the temperature beneath the 3 m thick active layer of the Murtèl rock glacier remains negative throughout the year. For example, temperatures recorded in a 11.6 m borehole at the Murtèl/Corvatsch rock glacier showed that the mean annual ground temperature generally increased from −2.3°C in 1987 to −1.4°C in 1994 with intermittent cooling during the interim years of 1994 to 1996 [*Vonder Müehll et al.*, 1998]. Permafrost in alpine rock glaciers, however, is relatively warm and typically tens of meters thick with temperatures that commonly vary around 0°C at depth. Considering the thermal inertia of ice-rich permafrost it is reasonable to assume that, in general, permafrost conditions have existed within alpine rock glaciers since the end of the last ice age [*Lunardini*, 1996]. The effects of snow cover may play an important role in regulating ground temperature and may likely influence the relations between the atmosphere and permafrost. To some degree, ventilation and cold air circulation within the blocky active layer also regulates the coupling between atmosphere and permafrost on mountain slopes and rock glacier surfaces [*Bernhard et al.*, 1998]. *Vonder Müehll*

et al. [1998] attribute the variability of observed permafrost temperatures to summer radiation and air temperature influences on the active layer, snow cover history, and shortened periods of negative temperatures during autumn months. Although the contribution and magnitude of these effects are likely to be significantly different on Mars, it is expected that they do play an important role in the preservation and location of water within viscous flow features there.

[45] A model of ice stability formulated by *Farmer and Doms* [1979] suggests that anywhere temperatures in the top 10 m of the Mars regolith exceed 198°K, ground ice will become unstable and can sublime and diffuse into the atmosphere. Thermodynamic models by *Clifford and Hillel* [1983] and *Mellon and Jakosky* [1995] produced similar results suggesting an ice-free region between ±30° latitude. Our study shows that a blocky debris mantle 1–5 m thick insulates the Yankee Boy rock glacier during summer months. The mantle also serves as an interchange for compacting snow that accumulates in the winter months (Figure 14). In cases where appreciable amounts of rock detach from a headwall or escarpment, a much thicker debris cover could be attained. For example, terrestrial rock glacier mantles of 1–10 m are not uncommon [*Clark et al.*, 1994]. Martian analogs, which are generally an order of magnitude larger than terrestrial rock glaciers, may have debris mantles that are considerably thicker. Using shadow lengths, *Squyres* [1988] estimated thicknesses between 500 and 900 m for debris aprons ranging in radial length from several kilometers to >15 km. A mantle of such thickness may be sufficient to preserve interstitial water ice or ice lenses long enough to achieve the type of flow length observed in landforms situated poleward of ±30° latitude on Mars.

[46] In a study of ice flow characteristics on Mars, *Colprete and Jakosky* [1998] used a simple model based on Glen's flow law to demonstrate the effects of ice temperature, accumulation rate, and purity on ice flow velocities in viscous flowing landforms:

$$\sigma_{xy} = A\tau_{xy}^{n} \tag{2}$$

$$A(T) = A_0\left(-\frac{Q}{RT}\right) \tag{3}$$

$$A(T) = 2.207 \times 10^{-5}\left[\frac{3155}{T} - \frac{0.16612}{(273.39 - T)^{1.17}}\right]^{n} \tag{4}$$

where: equation (2) represents the relation between shear strain rate (σ) and shear stress (τ). The coefficient A and exponent n represent the dependence on ice temperature, crystal orientation, impurity and other factors. $A(T)$ is the variation of coefficient A with respect to temperature (measured in Kelvins) according to the Arrhenius relation, where A_o is the temperature independent constant, R is the universal gas constant, and Q is the activation energy for creep [*Paterson*, 1994]. Equation (4) is an empirical relation developed by *Hooke et al.* [1972] for $A(T)$ across all temperatures below freezing.

[47] Results by *Colprete and Jakosky* [1998] suggest that ice temperatures must be greater than 220°K, and the net ice accumulation rate >1 cm/yr to produce the smallest observed rock glaciers. They calculated that at this temperature and accumulation rate it would take $\sim 10^6$ years to produce a 15-km flow, which is the average size flow observed on Mars. It was further concluded that formation times greater than 10^6 years are unlikely based on the climate fluctuations caused by variations in planetary obliquity and inclination [*Mellon and Jakosky*, 1995]. Ice held only in debris voids (i.e., at saturation or below) will have high yield strength and creep rates will be very low, if it occurs. Thus, ice within a body of debris will contribute to movement only when contained in lenses or similar masses. Furthermore, creep will only occur when these lenses or masses are interconnected or highly contiguous.

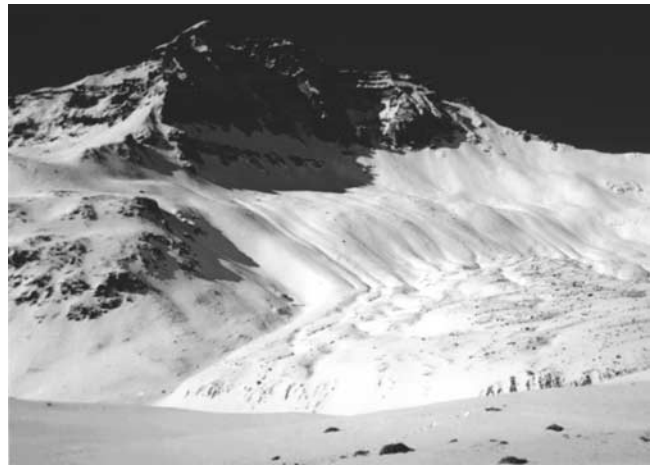

Figure 14. Snow covered rock glacier at Yankee Boy Basin. Seasonal layers of snow are most persistent in the accumulation zone. Permafrost is generated by accumulation and compaction of snow in the active layer of the rock glacier. Compaction occurs as the snow is buried by high magnitude episodes of rockfall and/or debris fall.

[48] If it is accepted that lobate debris aprons are commonly comprised of ice-cemented soils or ice-debris mixtures [e.g., *Squyres*, 1988; *Carr*, 1995], then consideration must be given to the condition that small concentrations of solid impurities in interstitial ice (at temperatures below 220°K) would reduce the flow velocities of Martian rock glaciers by an order of magnitude. For ice impurities of 30% or greater, flow velocities are so low that the time required for ice to reach the length of the features observed would exceed 10 Myrs [*Colaprete and Jakosky*, 1998]. Considering this discrepancy in flow rate versus landform size, a less viscous (i.e., soluble) component may be strongly affecting the rheology of the ice. Such a component is needed to generate large viscous flow features such as those observed under current Martian conditions (surface temperatures around 200°K for frost and accumulation rates of ~1 cm/yr). Under certain climatic and cryolithospheric conditions, liquid water may be a sustainable component that contributes significantly to the overall deformation.

4.3. Role of Water

[49] Numerous major geologic features on Mars appear to have formed by the release of large volumes of water from beneath the surface. Based on our current state of knowl-

edge about the history of the planet in terms of water and ice, there is no obvious way that such a volume of water could have been lost from the planet since the development of these features [*Squyres et al.*, 1992]. Outflow channels, however, provide persuasive evidence that a large reservoir of groundwater was stored in the Martian crust throughout its first billion years of geologic history [*Baker*, 1982; *Carr*, 1986].

[50] Under the influence of gravity, groundwater will drain to saturate the lowest porous regions of the crust. A subpermafrost groundwater system is viable if the present inventory of H_2O on Mars exceeds the quantity required to saturate the pore volume of the cryolithosphere. Once the pore volume of the cryolithosphere has been saturated with ice, any additional subsurface H_2O will inevitably be stored as groundwater [*Squyres et al.*, 1992]. Estimates by *Clifford* [1993] and *Clifford and Parker* [2001] indicate that a planetary inventory of H_2O equivalent to a several hundred meter-deep global ocean may satisfy this condition. Given an exponential decline in crustal porosity with depth, a groundwater inventory equivalent to a 100-m global ocean would then be sufficient to create a global aquifer nearly 4.3 km deep, assuming reasonable values of surface porosity (20–50%) and an exponential decay constant of 2.82 km [*Clifford*, 1993]. This range of porosity values is consistent with estimates of the bulk porosity of Martian soil as analyzed by the Viking Landers [*Clark et al.*, 1976].

[51] The hydrologic characteristics of the Yankee Boy rock glacier substantiate the presence of a water table and networks of interconnected water pathways throughout the layers of permafrost within (Figure 15a). The input sources for these water systems include streams, meteoric water/snow/ice, valley side runoff, lake water, springs, and frost. In light of the evidence provided for outflow channels on Mars, and the close proximity with which lobate debris aprons and other viscous flow bodies occur to them, it is possible that a number of these water sources have contributed to the development of ice-rich landforms. Channels or tables of liquid water and pure water ice residing within the permafrost (i.e., cryolithospheric material) for finite periods of time may be capable of initiating or sustaining the rates of deformation demonstrated by the lobate debris aprons and rock glaciers on Mars. It may even be possible that the dominant source of ice within these landforms originated from the subsurface as liquid water. Ice formed by the recharge of liquid water originating at depth (e.g., from outflow channels) could conceivably compensate for the volumes of ice lost to ablation in latitudes between 30° and 60°. Current models of rock glacier formation do not account for such a process. Figure 15b provides a conceptualized model for the internal structure of a Martian rock glacier and possible sources of water ice based upon findings from the surrogate rock glacier at Yankee Boy Basin.

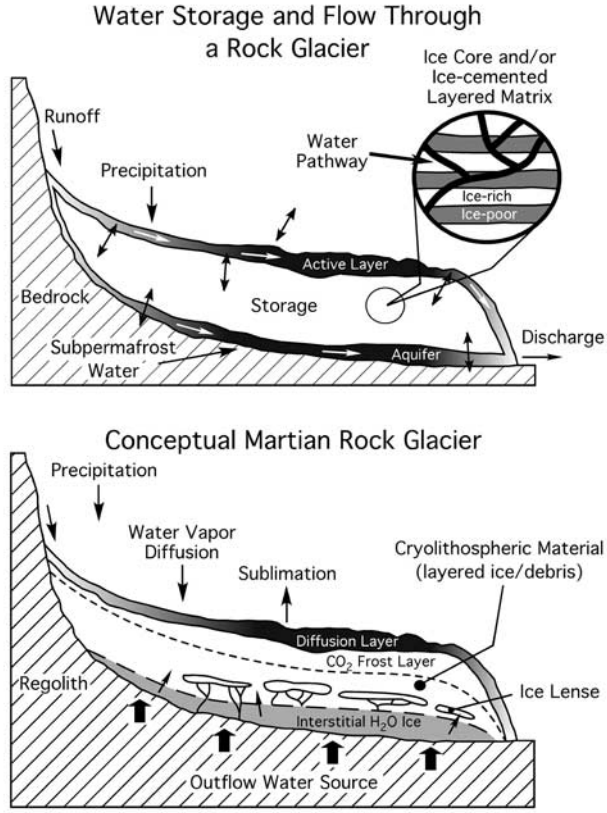

Figure 15. Diagrams illustrating (top) water storage and flow through a terrestrial rock glacier (modified from *Giardino et al.* [1992]) and (bottom) a conceptual Martian rock glacier based upon information obtained from terrestrial rock glaciers. Water entering the rock glacier system from outflow channel sources is transmitted upward through pore spaces, fractures, and zones of weakness. A network of water pathways is formed when the (warmer) water exploits pore spaces and melts through areas of weakness within the cryolithospheric material. The pathways terminate in lens-shaped pockets, with the remaining water forming an ice table at the base.

4.4. Flow Dynamics and Kinematic Properties

[52] Kinematic properties have been used to describe a variety of geomorphic systems including pool and riffle development, ice glacier surge, distributed streamflow, and slow mass movement [*Langbein and Leopold*, 1968; *Gerber and Scheidegger*, 1979]. Kinematic wave theory, as applied to glaciers [*Lighthill and Whitman*, 1955a, 1955b] and rock glaciers [*Olyphant*, 1987], requires that a wave of increased discharge (kinematic wave) travels down the rock glacier at a speed greater than the mean velocity of the surface [*Nye*, 1960]. The propagation of a kinematic wave can explain the discrepancies observed in rock glacier movement (rate and distance) as compared to talus supply rate [*Birkeland*, 1973; *Miller*, 1973; *White*, 1987]. Such a mechanism also allows for a disproportionally high rate of movement in the toe of a rock glacier with little or no increase in talus supply rate at the head. Thus, rheologic properties that govern movement may not control morphological development of the landform (i.e., kinematic wave motion may control form development even though mass and force control movement potential). Further, such development may be independent of variations in the driving forces responsible for the overall rheological properties [*Giardino and Vitek*, 1988a].

[53] The layering exhibited in the Yankee Boy rock glacier is not consistent with glacial and periglacial models

that call for deformation exclusively by faulting or surface-relegated folding [e.g., *Whalley et al.*, 1983; *Johnson*, 1984]. The depth of folding within the rock glacier indicates that energy is being transmitted through the major depositional units comprising the landform (i.e., through a succession of flow lobes), and not preferentially along the upper or lower portions. *Haeberli* [1985] notes that the surface of a rock glacier will deform into sequences of folds when: (1) compression develops parallel to the flow direction and (2) viscosity decreases downward from the surface of the rock glacier to the interior of the mass. The geometry of distinctive ridges and furrows and the internal structure observed at Yankee Boy suggests that folding is linked to propagation of the rock glacier. Currently, the most accepted model for the deformation of a rock glacier (i.e., Glen's Flow Law creep), does not take into account this type of folding. Efforts to refine the flow model must account for this internal structure, and considerations involving the movement of viscous-flow features on Mars should also include this phenomenon [*Degenhardt and Giardino*, 1999a, 1999b].

5. Summary and Conclusions

[54] Rock glacier-like features on Mars suggest the presence of flowing, or once-flowing ice-rock mixtures. These landforms, which include lobate debris aprons, concentric crater fill and lineated valley fill, hold significant promise as reservoirs of stored water ice that could be useful for human exploration of Mars. They may also contain frozen records of the climatic history of the planet. As such, it is important to understand the deformation and distribution of ice within these landforms. Using terrestrial rock glaciers as surrogates, we can apply the knowledge gained about internal structure, landform morphology, viscous flow properties, and the role of water to learn about the formation, internal character and deformation processes of Martian analogs.

[55] Results obtained from the rock glacier at Yankee Boy Basin show that the landform is comprised of distinct, continuous alternating ice-rich and ice-poor layers. Folds in the layers correspond to the surface expression of ridges and furrows, indicating that compressive stresses originating in the accumulation zone are transmitted downslope through the rock glacier. Thus, ridge-furrow topography is interpreted to be a surface manifestation of this process. Rock glacier features on Mars may also consist of layered permafrost ice and ice lenses, which would suggest a history of permafrost development involving seasonal frost accumulation and/or water influx from below the surface. Based on estimated thickness of lobate debris aprons and valley fill, and given the current climate and atmospheric conditions on Mars, mantle insulation may be sufficient to preserve water ice within these landforms.

[56] Liquid water, found to be abundant in the Yankee Boy rock glacier, occurs as a network of interconnected channels that permeate throughout the landform. In terms of water storage within Martian analogs, considerations must include the possibility that some water ice may be stored in relatively pure form within lenses and vein networks such as observed in the Yankee Boy rock glacier. Proximity of viscous-flow features to outflow channels indicates that a plentiful supply of water once flowed on the surface of Mars. If the total water budget of Mars exceeds the amount of ice stored within the Martian regolith, then the presence of liquid water beneath the surface is probable. Subterranean water could serve to replenish or to maintain the content of ice within Martian rock glaciers, thus providing a mechanism to perpetuate their flow for periods of time necessary to account for their size given current temperatures. Such water ice could be preserved within debris mantles of sufficient thickness, particularly if the mantles contain an insulating layer of frozen CO_2.

[57] Results of our work are also being used to test the concept of kinematic wave theory as applied to the dynamics of rock glacier movement. A kinematic wave model is appropriate because it considers motion and does not rely on the influences of mass and force, parameters that are poorly understood given the current knowledge of rock glaciers. Such evidence provides a better foundation for the use of rheological models that are required if rock glaciers are to be used as surrogates for evaluating water sources on Mars.

[58] This work is an important step toward understanding the fundamental development processes for rock glaciers. The flow dynamics of these and similar landforms can be understood only with knowledge of internal structure and composition. The results obtained in this study point toward the need for developing lighter and smaller remotely operated robotic GPR systems that can be sent to Mars. Development of lighter, more compact wireless systems should also be pursued for the eventual presence of human visitors to the planet.

[59] **Acknowledgments.** This work was made possible by a grant from the NASA Mission to Mars Program, and NASA grant NAG9-807. A great deal of appreciation goes to Brian Junck of the University of Calgary and Michael Quintana and Carl Pierce of Texas A&M University for their assistance in the field and for data processing. Dick Marston, Chris Neel and Mike Neel of Oklahoma State University also gave valuable time and effort to collecting topographic data and assisting with the radar equipment. Special thanks also to James Free, District Ranger, U. S. Department of Agriculture - Forest Service, for granting permission to conduct the research in the Uncompaghre National Forest, and particularly for the valuable assistance of Maureen McCormack and Ron Trujillo of the Ouray Ranger District Offices in Montrose and Ouray, Colorado.

References

Annan, A. P., and J. L. Davis, Impulse radar sounding in permafrost, *Radio Sci.*, *11*, 383–394, 1976.

Baker, V. R., *The Channels of Mars*, 198 pp., Univ. of Tex. Press, Austin, 1982.

Barsch, D., Nature and importance of mass-wasting by rock glaciers in alpine permafrost environments, *Earth Surf. Processes*, *2*, 231–245, 1977.

Barsch, D., Rock glaciers—Indicators for the present and former geoecology, in *High Mountain Environments*, pp. 76–82, Springer-Verlag, New York, 1996.

Bernhard, L., F. Sutter, W. Haeberli, and F. Keller, Processes of snow/permafrost-interactions at a high-mountain site, Murtèl/Corvatsch, Eastern Swiss Alps, in *Proceedings of the Seventh International Conference on Permafrost, Yellowknife, Canada*, *Collect. Nordicana*, *57*, 35–41, 1998.

Berthling, I., B. Elzelmuller, K. Isaksen, and J. L. Sollid, Rock glaciers on Prins Karls Forland, II, GPR soundings and the development of internal structures, *Permafrost Periglacial Processes*, *11*, 357–369, 2000.

Birkeland, P. W., Use of relative age dating methods in a stratigraphic study of rock glacier deposits, Mt. Sopris, Colorado, *Arctic Alp. Res.*, *5*(4), 401–416, 1973.

Brown, W. H., A probable fossil glacier, *J. Geol.*, *33*, 464–466, 1925.

Burger, K. C., J. J. Degenhardt Jr., and J. R. Giardino, Engineering geomorphology of rock glaciers, in *Changing the Face of Earth: Engineering Geomorphology: Proceedings of the 28th Binghamton Symposium in*

Geomorphology, edited by J. R. Giardino, R. A. Marston, and M. Morisawa, pp. 93–132, Elsevier Sci., New York, 1999.

Calkin, P. E., D. S. Kaufman, B. J. Przybyl, W. B. Whitford, and B. J. Peck, Glacier regimes, periglacial landforms, and Holocene climate change in the Kigluaik Mountains, Seward Peninsula, Alaska, USA, *Arctic Alp. Res.*, *30*(2), 154–165, 1998.

Carr, M. H., Mars a water-rich planet?, *Icarus*, *68*, 187–216, 1986.

Carr, M. H., Mars: A water-rich planet, in *MECA Symposium on Mars: Evolution of Its Climate and Atmosphere*, edited by V. Baker et al., pp. 23–25, Lunar and Planet. Inst., Houston, Tex., 1987.

Carr, M. H., The Martian drainage system and the origin of valley networks and fretted channels, *J. Geophys. Res.*, *100*, 7479–7507, 1995.

Clark, B. C., A. K. Baird, H. J. Rose, P. Toulmin III, K. Keil, A. J. Castro, W. C. Kelliher, C. D. Rowe, and P. H. Evans, Inorganic analysis of Martian surface samples at the Viking landing sites, *Science*, *194*, 1283–1288, 1976.

Clark, D. H., M. M. Clark, and A. R. Gillespie, Debris-covered glaciers in the Sierra Nevada, California, and their implications for snowline reconstructions, *Quat. Res.*, *41*, 139–153, 1994.

Clark, D. H., E. J. Steig, N. Potter Jr., J. Fitzpatrick, A. B. Updike, and G. M. Clark, Old ice in rock glaciers may provide long-term climatic records, *Eos Trans. AGU*, *77*(23), 217, 221–222, 1996.

Clifford, S. M., A model for the hydrologic and climatic behavior of water on Mars, *J. Geophys. Res.*, *98*, 10,973–11,016, 1993.

Clifford, S. M., and D. Hillel, The stability of ground ice in the equatorial regions of Mars, *J. Geophys. Res.*, *88*, 2456–2474, 1983.

Clifford, S. M., and T. J. Parker, The evolution of the Martian hydrosphere: Implications for the fate of a primordial ocean and the current state of the northern plains, *Icarus*, *154*, 40–79, 2001.

Colprete, A., and B. M. Jakosky, Ice flow and rock glaciers on Mars, *J. Geophys. Res.*, *103*(E3), 5897–5909, 1998.

Corte, A. E., Rock glacier taxonomy, in *Rock Glaciers*, edited by J. R. Giardino, J. F. Shroder Jr., and J. D. Vitek, pp. 27–39, Allen and Unwin, Concord, Mass., 1987.

Daniels, D. J., *Surface Penetrating Radar*, *IEEE Radar Sonar Navig. Avionics*, *6*, 300 pp., 1996.

Daniels, D. J., D. J. Gunton, and H. F. Scott, Introduction to subsurface radar, *Proc. IEEE*, *135*(part F4), 277–320, 1988.

Degenhardt, J. J., Jr., and J. R. Giardino, Kinematic wave models for Martian landforms based on rock glacier analogs, *Meteorit. Planet. Sci.*, *34*(4), suppl., A31, 1999a.

Degenhardt, J. J., Jr., and J. R. Giardino, Describing lobate Martian landforms using a terrestrial rock glacier kinematic wave model, *Geol. Soc. Am. Abstr. Programs*, *31*, A175, 1999b.

Degenhardt, J. J., Jr., and J. R. Giardino, GPR survey of a lobate rock glacier in Yankee Boy Basin, Colorado, USA, in *Ground Penetrating Radar* (*GPR*) *in Sediments: Applications and Interpretation*, edited by C. Bristow and H. Jol, in press, Geol. Soc. of London, London, England, 2003.

Degenhardt, J. J., Jr., J. R. Giardino, M. B. Junck, M. P. Quintana, and R. A. Marston, Evaluating the internal structure of a rock glacier using ground penetrating radar (GPR): Yankee Boy Basin, CO, USA, *Geol. Soc. Am. Abstr. Programs*, *32*(7), A516, 2000.

Degenhardt, J. J., Jr., J. R. Giardino, and C. Pierce, Longitudinal survey of a lobate rock glacier using ground penetrating radar (GPR), Yankee Boy Basin, CO, USA, *Geol. Soc. Am. Abstr. Programs*, *33*(6), A65, 2001.

Evin, M., Lithology and fracturing control of rock glaciers in southwestern Alps of France and Italy, in *Rock Glaciers*, edited by J. R. Giardino, J. F. Shroder Jr., and J. D. Vitek, pp. 83–106, Allen and Unwin, Concord, Mass., 1987.

Farmer, C. B., and P. E. Doms, Global and seasonal variation of water vapor on Mars and the implications for permafrost, *J. Geophys. Res.*, *84*, 2881–2888, 1979.

Fitzgerald, J. W., Morpho-dynamic modeling of rock glaciers: San Juan Mountains, Colorado, USA, Ph.D. dissertation, 202 pp., Texas A&M Univ., College Station, 1994.

Gerber, E. K., and A. E. Scheidegger, Systematics of geomorphic surfaces and kinematics of movements thereon, *Z. Geomorphol. N. F.*, *23*(1), 1–12, 1979.

Giardino, J. R., Rock glacier mechanics and chronologies: Mt. Mestas, Colorado, 244 pp., Univ. of Nebr., Lincoln, 1979.

Giardino, J. R., Movement of ice-cemented rock glaciers by hydrostatic pressure: An example from Mt. Mestas, Colorado, *Z. Geomorphol. N. F.*, *27*, 297–310, 1983.

Giardino, J. R., and J. D. Vitek, Rock glacier rheology: A preliminary assessment, in *Proceedings of the Fifth International Conference on Permafrost*, edited by K. Senneset, pp. 744–748, Trondheim, Norway, 1988a.

Giardino, J. R., and J. D. Vitek, The significance of rock glaciers in the glacial-periglacial landscape continuum, *J. Quat. Sci.*, *3*(1), 97–103, 1988b.

Giardino, J. R., J. F. Shroder, and J. D. Vitek, *Rock Glaciers*, 355 pp., Allen and Unwin, Concord, Mass., 1987.

Giardino, J. R., J. D. Vitek, and J. L. Demorett, A model of water movement in rock glaciers and associated water characteristics, in *Periglacial Geomorphology*, edited by J. C. Dixon and A. D. Abrahams, pp. 159–184, John Wiley, New York, 1992.

Haeberli, W., Creep of mountain permafrost: Internal structure and flow of alpine rock glaciers, *Mitt. Versuchsanst. Wasserb. Hydrol. Glaziol., 77*, 183 pp., 1985.

Haeberli, W., Modern research perspectives relating to permafrost creep and rock glaciers, *Permafrost Periglacial Processes*, *11*, 290–293, 2000.

Haeberli, W., and D. Vonder Müehll, On the characteristics and possible origins of ice in rock glacier permafrost, *Z. Geomorphol. N. F.*, *104*, suppl., 43–57, 1996.

Haeberli, W., J. Huder, H. Keusen, J. Pika, and H. Röthlisberger, Core drilling through rock glacier permafrost, *Proceedings of the Fifth International Conference on Permafrost*, *2*, 937–942, 1988.

Haeberli, W., M. Hoelze, A. Kääb, F. Keller, D. Vonder Müehll, and S. Wagner, Ten years after drilling through the permafrost of the active rock glacier Murtèl, Eastern Swiss Alps: Answered questions and new perspectives, *Proceedings of the Seventh International Conference on Permafrost, Yellowknife, Canada*, *Collect. Nordicana*, *57*, 403–410, 1998.

Haeberli, W., A. Kääb, S. Wagner, D. Vonder Müehll, P. Geissler, J. N. Haas, H. Glatzel-Mattheier, and D. Wagenbach, Pollen analysis and C^{14} age of moss remains in a permafrost core recovered from the active rock glacier Murtèl-Corvatsch, Swiss Alps: Geomorphological and glaciological implications, *J. Glaciol.*, *45*(149), 1–8, 1999.

Hooke, R. le B., B. B. Dalin, and M. T. Kauper, Creep of ice containing dispersed fine sand, *J. Glaciol.*, *11*, 327–336, 1972.

Horvath, C. L., An evaluation of ground penetrating radar for investigation of palsa evolution, Macmillan Pass, NWT, Canada, in *Proceedings of the Seventh International Conference on Permafrost, Yellowknife, Canada*, edited by A. G. Lewkowicz and M. Allard, *Collect. Nordicana*, *57*, 473–478, 1998.

Humlum, O., Origin of rock glaciers from Mellemfjord, Disko Island, Central West Greenland, *Permafrost Periglacial Processes*, *7*, 361–380, 1996.

Humlum, O., Active layer thermal regime at three rock glaciers in Greenland, *Permafrost Periglacial Processes*, *8*, 383–408, 1997.

Humlum, O., Rock glaciers on the Faeroe Islands, the North Atlantic, *J. Quat. Sci.*, *13*(4), 293–307, 1998.

Isaksen, K., R. S. Odegard, T. Eiken, and J. L. Sollid, Composition, flow and development of two tongue-shaped rock glaciers in the permafrost of Svalbard, *Permafrost Periglacial Processes*, *11*(3), 241–257, 2000.

Johnson, P. G., Rock glacier types and their drainage systems, Grizzly Creek, Yukon Territory, *Can. J. Earth Sci.*, *15*, 1496–1507, 1978.

Johnson, P. G., Rock glaciers: A case for a change in nomenclature, *Geogr. Ann.*, *65A*, 27–34, 1983.

Johnson, P. G., Rock glacier formation by high-magnitude low-frequency slope processes in the southwest Yukon, *Ann. Assoc. Am. Geogr.*, *74*(3), 408–419, 1984.

Jol, H. M., and D. G. Smith, Ground penetrating radar surveys of peatlands for oilfield pipelines in Canada, *J. Appl. Geol.*, *34*(2), 109–123, 1995.

Kaeaeb, A., W. Haeberli, and G. H. Gundmundsson, Analysing the creep of mountain permafrost using high precision aerial photogrammetry: 25 years of monitoring Gruben rock glacier, Swiss Alps, *Permafrost Periglacial Processes*, *8*, 408–426, 1997.

Langbein, W. B., and L. B. Leopold, River channels, bars and dunes—Theory of kinematic waves, *U.S. Geol. Survey Prof. Pap.*, *122L*, L1–L20, 1968.

Lehmann, F., D. Vonder Mühll, M. van der Veen, P. Wild, and A. Green, True topographic 2-D migration of geo-radar data, in *Proceedings of the Symposium on the Application of Geophysics to Environmental and Engineering Problems* (*SAGEEP*), edited by R. S. Bell, M. H. Powers, and T. Larson, pp. 107–114, Environ. and Eng. Geophys. Soc., Wheat Ridge, Colo., 1998.

Lighthill, M. J., and G. B. Whitman, On kinematic waves, I, Flood movement in long rivers, *Proc. R. Soc. London, Ser. A*, *222*, 281–316, 1955a.

Lighthill, M. J., and G. B. Whitman, On kinematic waves, II, A theory of traffic flow on long crowded roads, *Proc. R. Soc. London, Ser. A*, *222*, 317–345, 1955b.

Lucchitta, B. K., Ice and debris in the fretted terrain, Mars, *Proc. Lunar Planet. Sci. Conf. 14th*, Part 2, *J. Geophys. Res.*, *89*, suppl., B409–B418, 1984.

Lucchitta, B. K., Water and ice on Mars: Evidence from Valles Marineris, in *MECA: Papers Presented to the Symposium on Mars: Evolution of Its Climate and Atmosphere*, *LPI Contrib. 599*, pp. 59–61, Lunar and Planet. Inst., Houston, Tex., 1986.

Lucchitta, B. K., Mars: Periglacial and glacial forms of relief, in *Studies of the Quaternary Period: Selected Papers From the XI INQUA Congress*,

edited by I. P. Kartashov and K. V. Nikiforova, pp. 183–193, Izd. Nauka, Moscow, 1993.

Luedke, R. G., and W. S. Burbank, Map showing types of bedrock and surficial deposits in the Telluride Quadrangle, San Miguel, Ouray, and San Juan counties, Colorado, *U.S. Geol. Surv. Misc. Invest. Ser., Map I-973-A*, 1976.

Lunardini, V. J., Climatic warming and the degeneration of warm permafrost, *Permafrost Periglacial Processes*, *7*(4), 311–320, 1996.

Malin, M. C., K. S. Edgett, S. D. Davis, M. A. Caplinger, E. Jensen, K. D. Supulver, J. Sandoval, L. Posiolova, and R. Zimdar, Malin Space Science Systems Mars Orbiter Camera Image Gallery, Image M07-02044, San Diego, Calif., 16 Oct. 2000. (http://www.msss.com/moc_gallery/)

Malin, M. C., K. S. Edgett, S. D. Davis, M. A. Caplinger, E. Jensen, K. D. Supulver, J. Sandoval, L. Posiolova, and R. Zimdar, Malin Space Science Systems Mars Orbiter Camera Image Gallery, Image M19-01420, San Diego, Calif., 8 Oct. 2001. (http://www.msss.com/moc_gallery/)

McMechan, G. A., R. G. Loucks, Z. Xiaoxian, and P. Mescher, Ground penetrating radar imaging of a collapsed paleocave system in the Ellenburger dolomite, central Texas, *J. Appl. Geophys.*, *39*(1), 1–10, 1998.

Mellon, M. T., and B. M. Jakosky, The distribution and behavior of Martian ground ice during past and present epochs, *J. Geophys. Res.*, *100*, 11,781–11,799, 1995.

Miller, C. D., Chronology of neoglacial deposits in the Northern Sawatch Range, Colorado, *Arctic Alp. Res.*, *5*, 385–400, 1973.

Morey, R. M., Detection of subsurface cavities by ground penetrating radar, *Highway Geol. Symp. Proc.*, *27*, 28–30, 1974.

Murray, T., D. L. Gooch, and G. W. Stuart, Structures within the surge front at Bakaninbreen, Svalbard, using ground-penetrating radar, *Ann. Glaciol.*, *24*, 122–129, 1997.

Nye, J. F., The response of glaciers and ice sheets to seasonal and climatic changes, *Proc. R. Soc. London, Ser. A*, *256*, 559–584, 1960.

Olyphant, G. A., Rock glacier response to abrupt changes in talus production, in *Rock Glaciers*, edited by J. R. Giardino, J. F. Shroder Jr., and J. D. Vitek, pp. 55–64, Allen and Unwin, Concord, Mass., 1987.

Palacios, D., and L. Vazquezselem, Geomorphic effects of the retreat of Jamapa glacier, Pico de Orizaba volcano (Mexico), *Geogr. Ann. Ser. A Phys. Geogr.*, *78A*(1), 19–34, 1996.

Paterson, W. S. B., *The Physics of Glaciers*, 3rd ed., Elsevier Sci., New York, 1994.

Potter, N., Jr., Ice-cored rock glacier, Galena Creek, northern Absaroka Mountains, Wyoming, *Geol. Soc. Am. Bull.*, *83*(10), 3025–3057, 1972.

Potter, N., Jr., E. J. Steig, D. H. Clark, M. A. Speece, G. M. Clark, and A. B. Updike, Galena Creek Rock Glacier revisited—New observations on an old controversy, *Geogr. Ann.*, *80A*, 251–266, 1998.

Reynolds, J. M., *An Introduction to Applied and Environmental Geophysics*, 796 pp., John Wiley, New York, 1997.

Roberts, M. C., J. P. Bravard, and H. M. Jol, Radar signatures and structure of an avulsed channel: Rhone River, Aoste, France, *J. Quat. Sci.*, *12*(1), 35–42, 1997.

Sandeman, A. F., and C. K. Ballantyne, Talus rock glaciers in Scotland—Characteristics and controls on formation, *Scot. Geogr. Mag.*, *112*(3), 138–146, 1996.

Sensors & Software, *PulseEKKO 100 Run Users Guide Ver.1.2*, Tech. Manual 25, Sensors & Software, Ontario, Canada, 1996.

Shakesby, R. A., A. G. Dawson, and J. A. Matthews, Rock glaciers, protalus ramparts and related phenomena, Rondane, Norway: A continuum of large-scale talus-derived landforms, *Boreas*, *16*, 305–317, 1987.

Smith, D. G., and H. M. Jol, Radar structure of a Gilbert-type delta, Peyto Lake, Banff National Park, Canada, *Sediment. Geol.*, *113*(3–4), 195–209, 1997.

Soderblom, L. A., C. D. Condit, R. A. West, B. M. Herman, and T. J. Kriedler, Martian planetwide crater distributions: Implications for geologic history and surface processes, *Icarus*, *22*, 239–263, 1974.

Squyres, S. W., Martian fretted terrain: Flow of erosional debris, *Icarus*, *34*, 600–613, 1978.

Squyres, S. W., Urey Prize Lecture: Water on Mars, *Icarus*, *79*, 229–288, 1988.

Squyres, S. W., and M. H. Carr, The distribution of ground ice on Mars, *Eos Trans. AGU*, *65*(45), 979, 1984.

Squyres, S. W., and M. H. Carr, Geomorphic evidence for the distribution of ground ice on Mars, *Science*, *231*, 249–253, 1986.

Squyres, S. W., S. M. Clifford, R. O. Kuzmin, J. R. Zimbelman, and F. M. Costard, Ice in the Martian regolith, in *Mars*, edited by H. H. Kieffer et al., pp. 523–554, Univ. of Ariz. Press, Tucson, 1992.

Tanaka, K. L., Geologic/geomorphologic map of the Chryse Planitia Region of Mars, scale 1:5,000,000, *U.S. Geol. Surv. Misc. Invest. Ser., Map I-2441*, 1995.

Ulriksen, C. P. V., Application of impulse radar to civil engineering, 175 pp., Geophys. Surv. Syst. Inc., Hudson, N. H., 1982.

Vonder Müehll, D., and E. E. Klingelé, Gravimetrical investigation of ice-rich permafrost within the rock glacier Murtèl-Corvatsch (Upper Engadin, Swiss Alps), *Permafrost Periglacial Processes*, *5*, 13–24, 1994.

Vonder Müehll, D., T. Stucki, and W. Haeberli, Borehole temperatures in Alpine permafrost, *Proceedings of the Seventh International Conference on Permafrost, Yellowknife, Canada*, *Collect. Nordicana*, *57*, 35–41, 1998.

Wahrhaftig, C., and A. Cox, Rock glaciers in the Alaska Range, *Geol. Soc. Am. Bull.*, *70*, 383–436, 1959.

Whalley, W. B., Rock glaciers and their formation as part of a glacier debris-transport system, *Geogr. Pap. 27*, 48 pp., Univ. of Reading, Reading, England, 1974.

Whalley, W. B., G. R. Douglas, and A. Jonsson, The magnitude and frequency of large rockslides in Iceland in the postglacial, *Geogr. Ann., Ser. A*, *65*, 99–110, 1983.

Whalley, W. B., C. F. Palmer, S. J. Hamilton, and J. E. Gordon, Ice exposures in rock glaciers, *J. Glaciol.*, *40*, 427, 1994.

White, S. E., Debris falls at the front of Arapaho rock glacier, Colorado Front Range, U.S.A., *Geogr. Ann.*, *53A*(2), 86–91, 1971.

White, S. E., Differential movement across transverse ridges on Arapaho rock glacier, Colorado, Front Range, USA, in *Rock Glaciers*, edited by J. R. Giardino, J. F. Shroder Jr., and J. D. Vitek, pp. 145–149, Allen and Unwin, Concord, Mass., 1987.

J. J. Degenhardt Jr. and J. R. Giardino, Office of Graduate Studies, Texas A&M University, 302 Williams Administration Building, MS 1113, College Station, TX 77843-1113, USA. (degenjj@tamu.edu)